

AD-A248 166



DESIGN OF A WARM X-RAY RADIATION
ENVIRONMENT FOR NUCLEAR WEAPONS EFFECTS
TESTING IN THE NOVA-UPGRADE FACILITY

THESIS

Jeffrey E. Malapit
Captain, US Army

AFIT/GNE/ENP/92M-7

DTIC
SELECTED
APR 01 1992
SBD

92-08142



DISTRIBUTION STATEMENT A
Approved for public release
Distribution Unlimited

DEPARTMENT OF THE AIR FORCE
AIR UNIVERSITY
AIR FORCE INSTITUTE OF TECHNOLOGY

Wright-Patterson Air Force Base, Ohio

92 3 31 095

AFIT/GNE/ENP/92M-7

**DESIGN OF A WARM X-RAY RADIATION
ENVIRONMENT FOR NUCLEAR WEAPONS EFFECTS
TESTING IN THE NOVA-UPGRADE FACILITY**

THESIS

**Jeffrey E. Malapit
Captain, US Army**

AFIT/GNE/ENP/92M-7

Approved for public release; distribution unlimited.

REPORT DOCUMENTATION PAGE

*Form Approved
OMB No. 0704-0188*

Public reporting burden for this collection of information is estimated to average 1 hour per response, including the time for reviewing instructions, searching existing data sources, gathering and maintaining the data needed, and completing and reviewing the collection of information. Send comments regarding this burden estimate or any other aspect of this collection of information, including suggestions for reducing this burden, to Washington Headquarters Services, Directorate for Information Operations and Reports, 1215 Jefferson Dr, Suite 1204, Arlington, VA 22202-4302, and to the Office of Management and Budget, Paperwork Reduction Project (0704-0188), Washington, DC 20503.

1. AGENCY USE ONLY (Leave blank)			2. REPORT DATE March 1992	3. REPORT TYPE AND DATES COVERED Master's Thesis
4. TITLE AND SUBTITLE Design of a warm x-ray radiation environment for Nuclear Weapons Effects Testing in the Nova Upgrade Facility			5. FUNDING NUMBERS	
6. AUTHOR(S) Jeffrey E. Malapit, CPT, US Army				
7. PERFORMING ORGANIZATION NAME(S) AND ADDRESS(ES) Air Force Institute of Technology, WPAFB, OH 45433-6583			8. PERFORMING ORGANIZATION REPORT NUMBER AFIT/GNE/ENP/92M-7	
9. SPONSORING/MONITORING AGENCY NAME(S) AND ADDRESS(ES) DNA (TDTR) 6801 Telegraph Rd Alexandria, VA 22310-3398			10. SPONSORING/MONITORING AGENCY REPORT NUMBER	
11. SUPPLEMENTARY NOTES				
12a. DISTRIBUTION STATEMENT Approved for public release; distribution unlimited.			12b. DISTRIBUTION CODE	
13. ABSTRACT (Maximum 200 words) <p>This engineering design project examined the creation of a radiation environment for warm x-ray effects testing in the Nova Upgrade laser facility. With the use of the MORSE Monte Carlo Code and the DABL69 Broad-group cross section library, the ignition of an inertial confinement fusion pellet using D-T fuel in a test cassette was modeled in the Nova Upgrade's target chamber. Various x-ray scattering materials were used in the test cassette to include enriched lithium hydride, polyethylene, liquid hydrogen, liquid helium, and liquid methane. The lithium hydride produced the best warm x-ray doses and least neutron dose. The predicted x-ray dose in silicon was $6.30 + 0.09$ kGy per MJ (630 krad/MJ) of warm x-ray yield with a peak dose rate of 2.3×10^{12} Gy/s per MJ (2.3×10^{14} rad/s per MJ). For a nominal 20 MJ D-T ICF pellet with a 1% warm x-ray yield, the dose is 1.38 kGy (138 krad) and the peak dose rate is 4.6×10^{11} Gy/s (4.6×10^{13} rad/s). When this result is compared with the existing warm x-ray NWET simulators (MBS and MBS(PI)), three orders of magnitude gain in dose and four orders of magnitude gain in dose rate are realized. Less than 1% of the total dose was due to neutrons.</p>				
14. SUBJECT TERMS Nuclear weapons effects testing, Nova, Nova Upgrade, warm x rays, ICF, inertial fusion, NWET			15. NUMBER OF PAGES 117	
			16. PRICE CODE	
17. SECURITY CLASSIFICATION OF REPORT Unclassified	18. SECURITY CLASSIFICATION OF THIS PAGE Unclassified	19. SECURITY CLASSIFICATION OF ABSTRACT Unclassified	20. LIMITATION OF ABSTRACT UL	

AFIT/GNE/ENP/92M-7

**DESIGN OF A WARM X-RAY RADIATION ENVIRONMENT FOR NUCLEAR
WEAPONS EFFECTS TESTING IN THE NOVA-UPGRADE FACILITY**

THESIS

Presented to the Faculty of the School of Engineering

of the Air Force Institute of Technology

Air University

**In Partial Fulfillment of the
Requirements for the Degree of
Master of Science in Nuclear Engineering**

Jeffrey E. Malapit, B.S., P.E.

Captain, US Army

March 1992



Accession For	
NTIS	IR&I
DTIC	TR
Unpublished	
JULY 1992	
By	
Distribution	
Availability	
Dist	Final Version Special
Approved for public release; distribution unlimited.	

Approved for public release; distribution unlimited.

Preface

Amazing events occurred within the last year; among those events are the dissolution of the Soviet Union, the unification of Germany, the swift victory over Iraq, reunification talks with the Koreas and the US economic confrontation with our one time strong ally, Japan. One main theme remains predictable throughout history; events are not predictable. Yet technology advances with time throughout the world. As peace between the superpowers spreads less fear of the nuclear threat, more nations continue to advance in acquiring nuclear weapons and their means to launch them. The world was amazed at the advances made by Iraq in their nuclear weapons program; they were just months away from fielding a working nuclear bomb.

Defeats suffered by nations always come to the unprepared. The acquisition of nuclear weapons technology by countries unfriendly to the US is inevitable. As much as people wish for nuclear weapons to go away, one cannot uninvent the bomb. But, we do have the means to acquire technology to protect ourselves against the bomb. The Strategic Defense Initiative (SDI) is a program designed for that. We must have the resolve to protect ourselves before others unfriendly to us can acquire the means to destroy us.

This thesis was an engineering design project for modifications to the planned Nova Upgrade at the Lawrence Livermore National Laboratory in conjunction with others from the national laboratories, private companies, and the Department of Defense. It is my hope that this work be put to use by students, scientists, or engineers, if not in the Nova Upgrade facility, then in the planned Laboratory Microfusion Facility. I have written out some of the trickier parts and concepts with references as a guide for future use by other students. It is also my hope that this work may contribute to the peace of this nation through its strength.

I would like to thank those who made this thesis project go smoothly. Thanks to Dave Marchant for many long hours and late nights sharing ideas and common work for both of our projects. Thanks to Glen Sjoden for proofreading my paper and ripping it to shreds, thus forcing me to embark on a major rewriting effort for the better. Thanks to Mike Tobin of the Lawrence Livermore National Laboratory, my fellow ex-Army engineer, for his cooperation in providing me with hard to get information and explaining to me in simple terms (Army terms) hard to understand concepts and even treating me as an intellectual equal. Thanks to Major Denis Beller, my thesis advisor, for the benefit of his expertise

and work in this area and his contagious enthusiasm in my work. Special thanks to my wonderful children, Julia and Erin, for being there for me during my study breaks to relieve the tension and frustration when that darn code just wouldn't run right; and to my precious wife, Gigi, for her love, understanding, and support through all of my most difficult challenges in the Army and in life. I thank her for not only being there for me, but for her unselfish understanding for the many times when I could not be there for her.

Jeffrey E. Malapit
Dayton, Ohio

Table of Contents

	Page
Preface.....	i
Table of Contents.....	iv
List of Figures.....	vi
List of Tables.....	vii
Abstract.....	viii
1. Introduction.....	1
Background.....	1
Photon and Neutron Radiation Effects on Systems.....	3
Problem and Scope.....	6
Approach.....	7
Organization of Presentation.....	9
2. Detailed Analysis.....	11
Facility Description.....	11
The ICF Pellet and Energy Distribution.....	13
Target Chamber Description.....	14
3. Design Concept and Theory.....	16
Test Cassette Configuration.....	16
X-ray Scatterer.....	17
Shadow Shield.....	21
Debris Shield.....	22
Cassette Can.....	22
4. The MORSE Monte Carlo Code and DABL 69 Library.....	23
Description of the Code.....	23
The User Written Routines.....	24
5. Design Model.....	26
Input Geometry Descriptions.....	26
Source: The Input Spectrum.....	26
X Rays.....	26
Neutrons.....	29
Materials.....	29
Detector Response Functions.....	29
6. Results and Discussion.....	31
Organization.....	31

Solid Scattering Material.....	32
Lithium Hydride.....	32
Polyethylene.....	35
Cryogenic Scattering Material.....	36
Hydrogen.....	36
Helium.....	37
Methane.....	39
Effect of Warm X-Ray Spectrum Temperature.....	39
Effect of the Capture Gamma Rays.....	40
The Effect of Apertures.....	43
Effect of Geometry Changes on Pulse Width.....	46
Comparison with Current Simulators.....	48
 7. Summary, Recommendations and Conclusions.....	50
Summary.....	50
Recommendations for Future Work.....	50
Conclusions.....	52
 Bibliography.....	53
 Appendix A: User Written Routines for MORSE.....	56
 Appendix B: Example of MORSE Data Input File.....	67
 Appendix C: Example of MORSE Data Output File.....	71
 Appendix D: Example of XCHECKER Data Input File.....	99
 Appendix E: Material Densities and Element Number Densities	101
 Appendix F: Photon Detector Response Functions.....	102
 Appendix G: Neutron Detector Response Functions.....	103
 Vita.....	104

List of Figures

Figure 1. Plan View of Nova Upgrade Target Chamber.....	12
Figure 2. Elevation View of Nova Upgrade Target Chamber...	12
Figure 3. Concept of the Final Beamlet Optics for the Nova Upgrade.....	13
Figure 4. Test Cassette Design Layout for the Nova Upgrade Target Chamber.....	17
Figure 5. Particle Fluence for a Lithium Hydride Scatterer	41
Figure 6. Silicon Response Functions for Photons and Neutrons.....	42
Figure 7. Neutron and Gamma Ray Dose Rates for Lithium Hydride Scatterer.....	43
Figure 8. Comparison of Varying Geometries to Lengthen Pulse Width.....	47

List of Tables

Table 1. Source Photon Spectrum Fractions and Total Source Photons.....	28
Table 2. Comparison of Dose and Dose Rate Values for Different X-Ray Scattering Materials in the Nova Upgrade for a 20 MJ D-T ICF Pellet.....	32
Table 3. Dose Values for Lithium Hydride Scatterer.....	33
Table 4. Dose Values for Lithium Hydride in 10 mils of Kapton.....	34
Table 5. Dose Values for a Polyethylene Scatterer.....	35
Table 6. Dose Values for a Liquid Hydrogen Scatterer.....	36
Table 7. Dose Values for a Liquid Helium Scatterer.....	37
Table 8. Dose Values for a Liquid Methane Scatterer.....	39
Table 9. Comparison of Dose in Silicon from Various Warm X-ray Blackbody Temperatures.....	40
Table 10. Comparison of Dose and Dose Rate Values for X-Ray Scattering Materials With Apertures Modeled.....	46
Table 11. Comparison of Current NWET Simulators and Predicted Radiation Environment in Nova Upgrade.....	48
Table 12: Material and Element Number Densities.....	101
Table 13: Photon Detector Response Functions.....	102
Table 14: Neutron Detector Response Functions.....	103

Abstract

This engineering design project examined the creation of a radiation environment for warm x-ray effects testing in the Nova Upgrade laser facility. With the use of the MORSE Monte Carlo Code and the DABL69 Broad-group cross section library, the ignition of an inertial confinement fusion pellet using D-T fuel in a test cassette was modeled in the Nova Upgrade's target chamber. Various x-ray scattering materials were used in the test cassette to include enriched lithium hydride, polyethylene, liquid hydrogen, liquid helium, and liquid methane. The lithium hydride produced the best warm x-ray doses and least neutron dose. The predicted x-ray dose in silicon was 6.30 ± 0.09 kGy per MJ (630 krad/MJ) of warm x-ray yield with a peak dose rate of 2.3×10^{12} Gy/s per MJ (2.3×10^{14} rad/s per MJ). For a nominal 20 MJ D-T ICF pellet with a 1% warm x-ray yield, the dose is 1.38 kGy (138 krad) and the peak dose rate is 4.6×10^{11} Gy/s (4.6×10^{13} rad/s). When this result is compared with the existing warm x-ray NWET simulators (MBS and MBS(PI)), three orders of magnitude gain in dose and four orders of magnitude gain in dose rate are realized. Less than 1% of the total dose was due to neutrons.

DESIGN OF A WARM X-RAY RADIATION ENVIRONMENT FOR NUCLEAR WEAPONS EFFECTS TESTING IN THE NOVA-UPGRADE FACILITY

1. Introduction

Background

The Nova Laser Facility at the Lawrence Livermore National Laboratory houses the Nova Laser. With the capability of focusing 120 kilojoules (kJ) of energy through its ten laser beams, the Nova Laser is currently the most powerful in the world. By the end of the decade, the planned Nova Upgrade will be able to focus two megajoules (MJ) of energy through 288 laser beamlets onto a target. The primary purpose of the Nova Upgrade is to prove that inertial confinement fusion (ICF) works. It will use its 2 MJ laser to drive ICF reactions in pellets to produce up to 30 MJ of fusion yield [Tobin et. al., 1991:1]. Although the Nova Upgrade's main purpose is to provide proof of principle that inertial confinement fusion will work, the resulting ignition of the fusion pellet inside Nova Upgrade's target chamber will create a unique radiation environment which can be useful for nuclear weapons effects testing (NWET).

This unique radiation environment is produced by the ICF reaction. The ignited ICF pellet will release energy in the form of neutrons, x rays, and debris. Neutrons comprise of 70% of the total fusion yield, x rays 15%, and debris 15%.

The x rays released will contain a peak in the warm x-ray region (between 10 and 100 keV) from the ignited D-T pellet. This warm x-ray peak will carry 1-5% of the total fusion yield. It is this warm x-ray peak that is of interest to the Defense Nuclear Agency (DNA) for NWET.

DNA points out a missing slice in the x-ray spectrum that is not produced at sufficient energy fluences in its current NWET simulators. This missing slice is in the warm x-ray region defined between 10 and 100 keV [Gullickson, 1991]. The following quote from the report on "Test Capabilities for Nuclear Hardened Space Systems" sums up the current situation:

...a breakthrough in the capability to generate warm photons is required; the current capability must be enhanced by about five orders of magnitude. The technology for this "Next Generation Machine" is not at hand, nor is the present R&D effort adequate to the task....[quoted by Gullickson, 1991].

However, the warm x rays created by the ICF reaction in the Nova Upgrade may provide sufficient energy fluences to fill this need and provide cheaper testing of devices or even sub-systems in environments that could only be achieved in more expensive underground testing [Kennedy, 1991]. The success of the Nova Upgrade in NWET can serve as a precursor for designs in the Laboratory Microfusion Facility (LMF), a larger facility that can test whole systems at larger test yields. The LMF is a proposed facility that will test high-

gain ICF pellets with fusion yields of 1 GJ with 10 MJ laser drivers. Properly configured, Nova Upgrade can demonstrate a clear advantage over existing NWET simulators for warm x-ray test requirements.

Photon and Neutron Radiation Effects on Systems

Current NWET simulators produce radiation to simulate the effects of nuclear weapons on critical government systems such as space vehicles or strategic weapon systems. The photon spectrum that is useful for NWET is generally divided into four regions by the NWET community. They define the regions based on general damage effects the photons cause on equipment and systems. First, cold x rays (below 10 keV) deposit their energy in a thin layer outside the material. This causes ablation and structural damage due to shock waves from the ablated material. Second, warm x rays (8-100 keV) cause thermostructural and electronic device damage. Thermostructural damage is caused by warm x rays depositing energy on only one side of the material which commonly causes materials to bend (called the banana effect). Electronic device damage is caused by warm x rays penetrating into semiconductors which causes upset and latch ups in internal electronic devices. Third, hot x rays (80 keV-800 keV) and fourth, gamma rays (greater than 800 keV) penetrate deep into a system and can interact directly with

internal electronic devices which causes upset and latch up, destroys devices through burn out, or causes system-generated electromagnetic pulse (SGEMP) [Gullikson, 1991] [Pressley, 1991] [Messenger and Ash, 1986:216-263]. The defined energy ranges overlap because different organizations define the photon ranges differently but generally within the above stated ranges.

The most important effects of fast neutrons on systems are on the electronics. Fast neutrons penetrate deep into systems which damages its internal components and, in sufficient fluences, causes changes in chemical properties. Since neutron fluences necessary to cause significant chemical effects are within ranges where blast and thermal effects of a nuclear weapon would dominate, the primary concern is on electronics. Neutrons can knock atoms out of semiconductor lattice structures which changes their operating characteristics or causes them to fail. In semiconductor devices there are positive (holes) and negative charge carriers (electrons). The lesser number of holes or electrons is the minority carrier. The ability of semiconductors to perform depends on the concentration of these charge carriers in various areas of the semiconductor. The performance of semiconductors can be measured in the number density and mobility of charge carriers and the number density and lifetime of minority charge carriers.

The three primary effects of the atomic displacement due to fast neutrons are an increase in trapping, scattering, and recombination centers in the semiconductors. The increase in trapping centers decreases charge carrier density, thus reducing current. The increase in scattering centers reduces charge carrier mobility. The last effect of the increase of recombination centers is the most important for bipolar devices; it reduces the time minority carriers are available for conduction which has the biggest impact on semiconductor performance [Messenger and Ash ,1986 :157-215] [Glasstone and Dolan, 1977:383-385].

The combined effects of neutrons and photons are difficult to predict in complex electronics or structural systems. The different radiations combine synergistically to produce damage in systems. Thus the testing of separate components of systems usually will not give the designer a true picture of the radiation effects in a whole system. Therefore, it is desirable to test complete systems under combined radiation environments to assess their vulnerabilities. This is usually done in underground testing (UGT). UGT is costly; cost estimates run about \$1 million per square foot of test area [Kennedy, 1991]. Therefore, it is desirable to test individual components or sub-systems separately to ensure as many of the more predictable effects are protected against prior to costly

UGT. DNA recommends maximum use of its above ground testing (AGT) simulators prior to UGT.

Presently, only two NWET facilities can produce fluences primarily in the warm x-ray region: the Modular Bremsstrahlung Source (MBS) at the Maxwell Laboratory and the MBS at the Physics International Laboratories (MBS-PI). Neither produces sufficient doses in the warm x-ray region that are currently needed. They produce doses in silicon about 3.5 Gy (0.35 krad) and dose rates around 10^7 Gy/s. For assessing photon damage, doses in the 1 to 100 kGy and dose rates about 10^9 Gy/s are required to test hardened devices and systems [Messenger and Ash, 1986:247-261, 294, 297].

Problem and Scope

The problem of this thesis is to design a structure to transport the resulting warm x-ray fluence from the ICF pellet while reducing the accompanying neutrons and their secondary gamma ray doses to a test zone. The reduction of neutron and gamma ray dose is necessary so that the damage caused by the warm x rays is readily apparent. The resulting x-ray spectrum on target should be in the warm x-ray region between 10 and 100 keV. Neutron dose contributions can be as high as 50% of the total dose, but preferably less than 10% [Kennedy, 1991]. If significant

warm x-ray doses and dose rates can be produced with ICF in the Nova Upgrade, the NWET ability for the warm x-ray test requirement could be greatly enhanced.

This project models the ICF pellet source of neutrons and x rays at a point source and tracks their interactions inside a model of a designed test cassette inserted inside the Nova Upgrade target chamber. The model was created using a Monte-carlo transport program and a broad-group library of photon and neutron group cross-sections. Various scatterer designs were made of materials with high cross section values for neutron absorption and x-ray scattering-to-absorption ratios. These materials should maximize the warm x-ray dose and minimize the neutron dose at the test zone. The dose in the test zone is modeled in silicon so that the results can be compared with current NWET simulators.

Approach

This design project followed a careful plan designed to build confidence in the results. The neutral particle transport code, MORSE, was used to predict radiation effects. A MORSE module called XCHECKER extracts cross section data to generate macroscopic cross sections for materials for defined energy bins prior to a transport code run which saves computational time. Another MORSE module

called PICTURE creates a printed view of the input geometry so that one can verify if the described configuration is adequately defined. MORSE is described further in Chapter 4. The steps taken were:

1. Coordinate with Nova Upgrade working group members on design limitations on the test cassette.
2. Compile and run the sample problems and code provided by ORNL and fix any problems discovered.
3. Determine and pre-mix cross section data required by the specific problem, with the use of the MORSE module XCHECKER.
4. Develop a simple geometry with the use MORSE module PICTURE to check user written routines.
5. Develop written routines to provide specific source and detector responses required by the specific problems.
6. Test the written routines modeling a single group input spectrum and simple geometries.
7. Develop specific geometries for the actual problems and verify with the use of the MORSE module PICTURE.
8. Develop input spectral data for both x-rays and neutrons, gamma-generation information (from the XCHECKER

run), and any KERMA (Kinetic Energy Released in Material) factors necessary.

9. Analyze materials used. Estimate weight, ablation depth, and impulse transferred from debris and x-ray ablation to estimate material disassembly.

10. Run the problem and examine results. Evaluate, alter the geometry and materials as necessary and rerun.

11. Run the most promising designs over a range of possible ICF source characteristics.

Organization of Presentation

The following chapters contain a detailed description of this project. Chapter 2 contains an analysis of the relevant features of the Nova Upgrade laser facility and the constraints on the design of the test cassette. Chapter 3 contains the theory behind the selection of materials and configurations used. Chapter 4 describes the transport code and cross section library used. It is written with the assumption of reader familiarity with neutral particle transport theory. Chapter 5 describes the actual geometries and materials modeled in the transport code. Chapter 6 contains the results of several selected designs and materials with a discussion. Finally, Chapter 7 presents

the summary, recommendations for future work, and the conclusions of this design project.

2. Detailed Analysis

Facility Description

The Nova Upgrade laser facility will consist of 288 laser beamlets surrounding a spherical target chamber and a target inserter extending through the top of the target chamber. The target chamber will be assembled in two hemispheres with the equator vertical. The laser beamlets will be angled toward the target chamber sideways around the poles in four belts at each side at 25° , 35° , 47° , and 57° half-angle cones (See figures 1,2 and 3). Each laser beamlet requires an unobstructed aperture from a point in the center of the target chamber to a 45-cm radius focal lens located 6.7 m away. This equates to a 1.9° half angle for each aperture. The 288 laser beamlets require 8% of the surface area of the target chamber. Additional test diagnostic apertures and a vacuum manifold require 2% more surface area [Tobin, 1991].

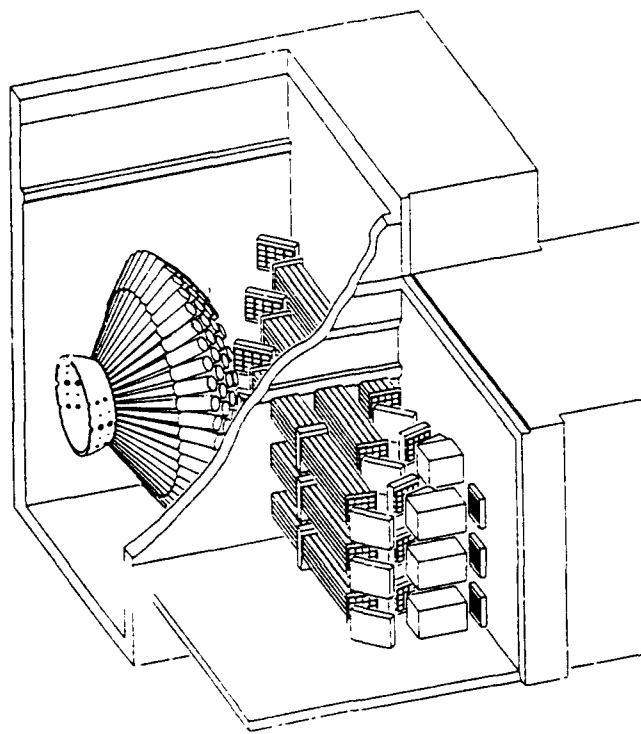


Figure 1. Plan view of beam layout around the Nova Upgrade target chamber.[Tobin, 1991]

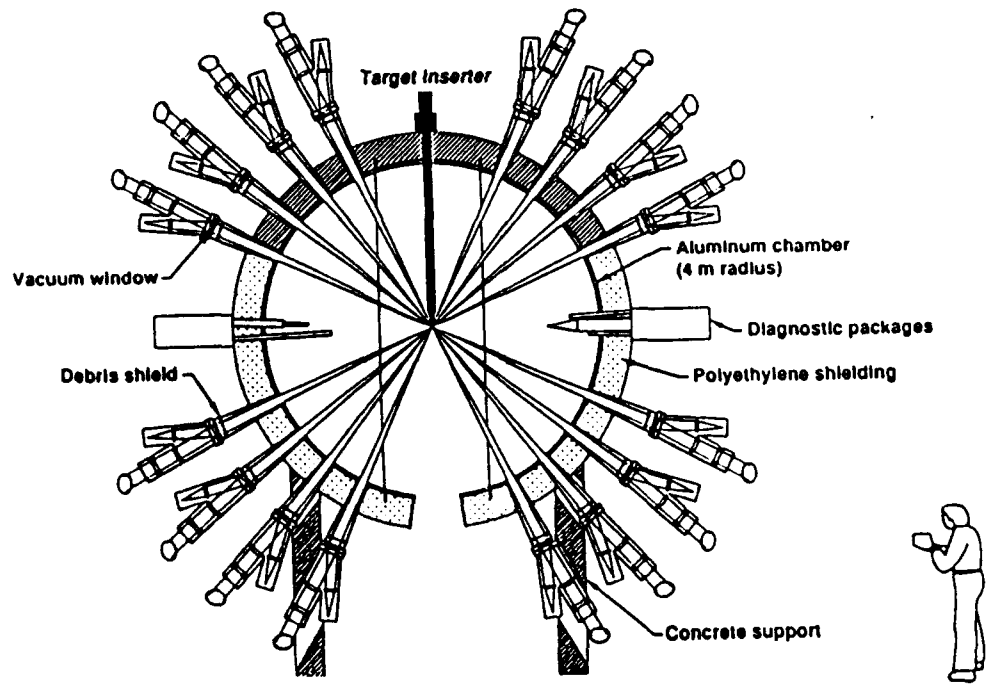


Figure 2. Elevation view of the Nova Upgrade target chamber area.[Tobin et. al., 1991:4]

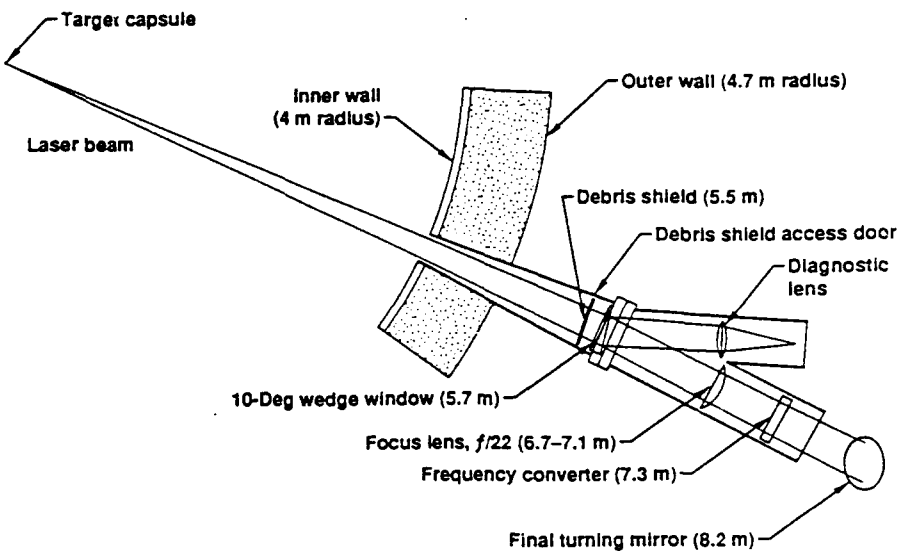


Figure 3. Concept of the Final Beamlet Optics for the Nova Upgrade.[Tobin et. al., 1991:9]

The ICF Pellet and Energy Distribution

The most promising ICF pellets use deuterium-tritium (D-T) fusion fuel. The pellet is encased in a thin high-Z material container called a hohlraum. The 288 laser beamlets deliver 2 MJ of energy into the sides of the hohlraum simultaneously, stimulating a high flux of very cold x rays below 1 keV. These cold x rays strike the pellet ablating the exterior. This uniform ablation creates shock waves which compresses the pellet sufficiently to cause the D-T fusion reaction to occur inside the pellet [Inertial Confinement Fusion, 1989:3,16]. The resulting fusion reaction releases x rays, neutrons, and debris into the target chamber. The energy from the fusion target and the laser driver is partitioned between the neutrons, debris

and x rays. The neutrons from the D-T reaction characteristically have an initial energy of 14.1 MeV [Krane, 1988:530]. The neutrons carry 70% of the total fusion energy. The debris from the pellet and hohlraum carry 15% of the fusion energy and 50% of the laser energy. The x rays comprise about 15% of the total fusion energy and 50% of the laser energy [Tobin et. al., 1991:3].

The x-ray energy is further distributed between two peaks. A cold x-ray peak is caused by the x-ray emissions of the high-Z hohlraum [Inertial Confinement Fusion, 1989:16]. A warm x-ray peak is caused by the burning D-T pellet and is modeled by a 6-10 keV blackbody spectrum. The 15% total x-ray energy from the fusion reaction is divided from 1-5% warm x rays and 10-14% cold x rays [Tobin, 1991]. All of the x-ray energy from the laser is in the cold x-ray peak [Tobin et. al., 1991:3]. For the nominal 20 MJ ICF pellet yield and 2 MJ laser energy considered, the neutrons carry 14 MJ of energy, the debris 4 MJ, the cold x rays 3 to 3.8 MJ, and the warm x rays 0.2 to 1 MJ.

Target Chamber Description

The Nova Upgrade target chamber will house the ICF pellet and contain the harmful radiation and debris after fusion ignition. The target chamber has a 4 meter inner radius. The first inner wall will be 5 cm of Aluminium

alloy 5083 that contains a low manganese content. This limits the build up of ^{54}Mn with its 312 day half-life. Encasing the inner wall is 20 cm of high density leaded borated polyethylene interlocking blocks that will shield prompt neutrons and gamma rays. The target chamber walls will also have 288 apertures for the laser beamlets to focus upon the target. When in operation, the target chamber will have only 10^{-5} torr of pressure inside [Tobin et. al., 1991:1-7].

Running through the top to the center of this target chamber will be the target inserter. It will be generally cylindrical in shape and have a 10 mm radius. It will suspend the target pellet in the center of the target chamber by kevlar filament support fibers. These fibers will vaporize when the ICF pellet ignites. The target inserter will also have liquid nitrogen and helium to keep the ICF pellet at a temperature of 15 K to allow easier compression from x-ray ablation. [Tobin et. al., 1991:7]

3. Design Concept and Theory

Test Cassette Configuration

Since most of the energy released from the fusion pellet is in the form of high-energy neutrons, cold x rays, and debris, some modification must be made to maximize the smaller percentage of warm x rays reaching the test area while minimizing the other fusion pellet products. To accomplish this a structure called a test cassette is necessary. The final design configuration of this proposed test cassette uses a hollow cylinder shaped cassette (a can) that is inserted into the bottom of the target chamber. Because of structural reasons of the target chamber, the maximum radius of the can is 75 cm [Tobin, 1991]. On the top of the can is a warm x-ray scatterer. Between the pellet and the test area is a shadow shield that prevents direct fusion pellet shine on the test area. A hibachi-supported debris shield protects the test area from shrapnel. The can walls support the scatterer and protect the test area from lateral debris and radiation (See figure 4). The test area is in the lower 2 meters of the can where the test components and the supporting diagnostic equipment can be stored. The test cassette is lifted into position and supported by an elevator.

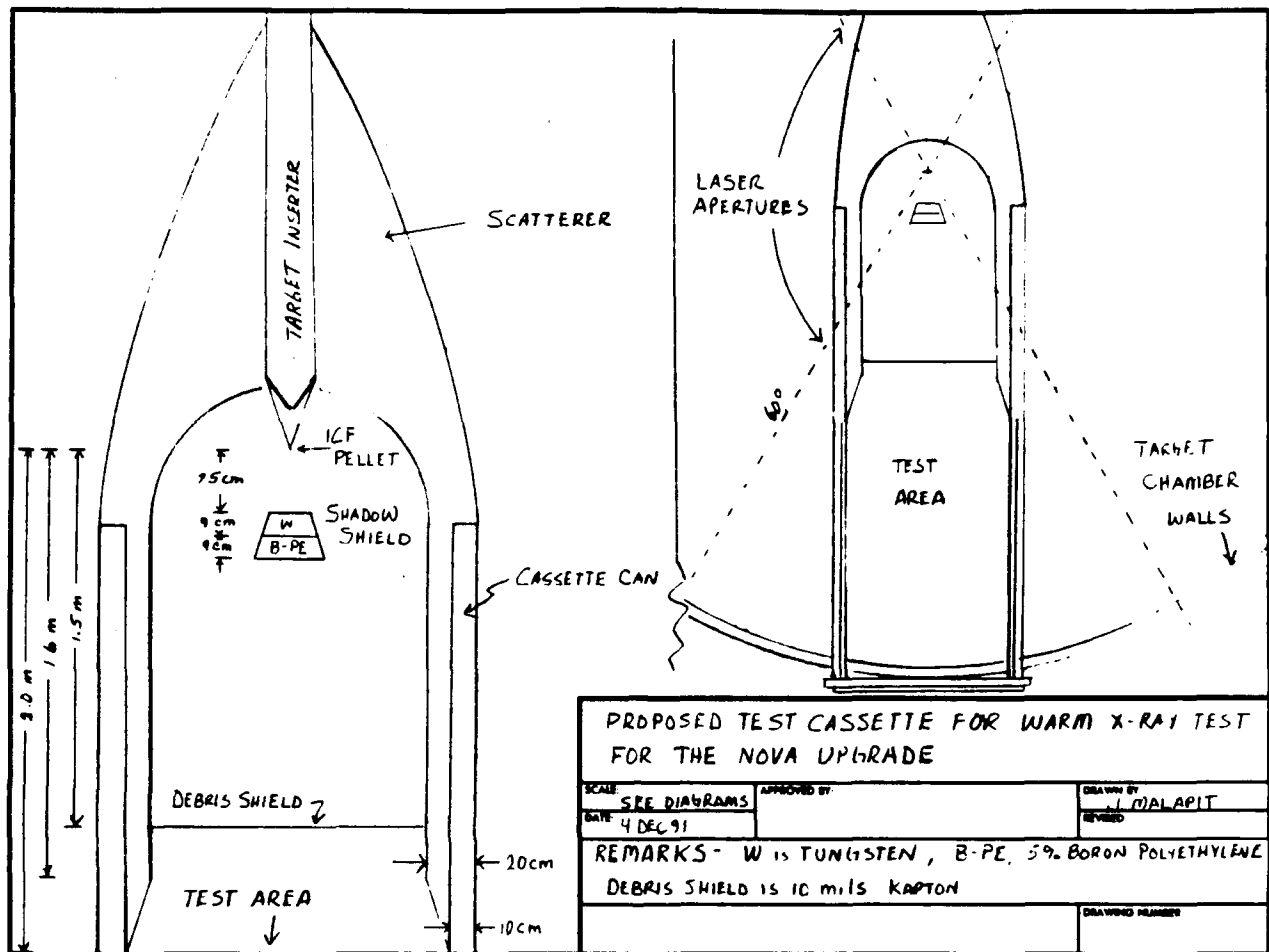


Figure 4. Test Cassette design layout for warm x-ray test in the Nova Upgrade.

X-ray Scatterer

The scatterer is a low-Z material, semi-elliptical shell with the open side facing downward toward the test area. The apex is 2 m from the source and its minor axis is 75 cm from the source (See Figure 4). The interior surface is spherical with a 55 cm radius and is 25 cm from the source. The scatterer also extends down to 2 m from the bottom of

the can in the shape of a 10 cm thick annulus. It must have beamlet apertures and another 10 cm radius opening at the top for the target inserter. The scatterer rests on the walls of the cassette can.

A low-Z material is necessary for the composition of the scatterer. The Klein-Nishina equation describes the scattering angles of photons. High energy photons tend to scatter forward. Low-energy photons scatter nearly isotropically. Low-Z atoms also have higher photon scatter-to-absorption ratios. Fast neutrons scatter anisotropically forward off low Z materials and near isotropically off higher-Z materials [Krane, 1988;201]. Using a low-Z material will then give the advantage of scattering the high energy neutrons forward out of the test cassette while reflecting the warm x rays toward the test area.

The lightest naturally occurring solid material is lithium hydride. Lithium hydride is manufactured in individual grains and pressed together to form desired shapes. Since it is highly hygroscopic, the grains are coated in a sub-micron layer of parylene (a polyimide film). The hydrogen and lithium are ideal for warm x-ray scattering when compared to other elements. The hydrogen is excellent for scattering the neutrons out of the test cassette. The lithium is excellent for suppression of capture gamma rays [Shielding and Foils, 1982:2,4].

For this design, the scatterer material consisted of lithium hydride enriched to 95.6% Li6 content. Natural lithium consists of 7.5% Li6 and 92.6% Li7. Because Li6 is lighter it scatters the neutrons better than the Li7. Enrichment to Li6 should improve neutron energy reduction.

Lithium hydride, however, is a difficult and hazardous material to work with. Clean up crews after each test shot face the difficult task of cleaning up disassembled lithium hydride debris. Encasing the lithium hydride in 250 microns (10 mils) of Kapton (Kapton is a registered tradename for DuPont's unique rugged polypyromellitimide film) should contain any spalling from the backside, but its integrity of the side facing the fusion ignition would have to be studied further [Seaman et. al., 1989:56]. The addition of Kapton (a monomer of Kapton is $C_{22}H_{18}O_5N_2$) to the scatterer will reduce the warm x-ray fluence on the test area and increase the neutron and secondary gamma ray dose. If lithium hydride proved to difficult for clean up, an alternate non-hazardous material is needed.

Polyethylene was tested because it is non-hazardous and has a very high density of hydrogen. Its monomer is C_2H_4 . Because of its carbon content, polyethylene is expected to give less warm x-ray dose and a higher neutron and gamma ray dose to the test area than lithium hydride would.

Other solid materials considered were beryllium hydride (BeH) and lithium boro-hydrate (LiBH_4). Beryllium hydride was just as hazardous as and offered no significant advantages over lithium hydride. Lithium boro-hydrate offered a higher hydrogen density than lithium hydride, but the high absorption cross section of boron suppressed warm x-ray dose at the test area too greatly.

Since low Z material is best for the scatterer, hydrogen and helium would make excellent scatterer materials. Low Z material with strength to hold the highly compressed hydrogen and helium gases is difficult to find. But a Kapton shell with a parylene vapor coating could contain liquid hydrogen and helium. Kapton maintains its strength even down to 4 K [Mark, 1964:268]. Even with liquid hydrogen and helium, a mean free path for warm x rays between 10-20 keV is about 40 cm. To configure more than one mean free path thickness hemispherically around the source pellet is difficult since the test cassette radius is limited to 75 cm. The Kapton absorbs many of the warm x rays and increases the neutron and gamma ray dose. The warm x rays that penetrate the Kapton scatter deep into the liquid hydrogen or helium scatterer which contributes less fluence to the test area. Liquid methane was also considered for its high hydrogen content plus it offers the advantage of not having to be cooled (boiling point at 112

K) to as low a temperature as hydrogen (20 K) and helium (5 K) Compressed Gas Association, 1990:388,395,461].

Shadow Shield

To protect the test region from the intense prompt neutron pulse and debris, a conical shadow shield is in the direct path to the test region. The neutron shield must be composed of neutron scattering and absorbing material. To protect the target chamber from shrapnel and neutron melt, no objects are placed closer than 25 cm from the target pellet. Hence, the neutron shield is 25 cm from the pellet and extends downward toward the test area which shields the lower 2 m of the can from direct shine. The shadow shield consists of 9 cm of tungsten and 9 cm of 5% borated-polyethylene which provides 4 mean free paths (3 mean free paths through tungsten and 1 mean free path through the B-polyethylene) for 14 MeV neutrons. The neutron shield must be supported by thin shock absorbers capable of dampening the shock from debris and x-ray ablation. Three thin polyethylene rods should provide adequate shock absorption.

Debris Shield

The debris shield is 254 microns (10 mils) of Kapton type H film. It is one of the toughest plastics and is known for its strength, thermal resistance, and radiation

resistance [Shrinet, 1982:556-557][Mark, 1964:265-269]. The Kapton shield filters out most x rays below 10 keV.

Cassette Can

The cassette can houses and shields the test components and supports the scatterer. It has a 75 cm outer and 65 cm inner radius. Approximately 144 laser apertures will be in the upper 1.4 m of the can. The lower 2 m of the can which protects the test area consists of 2.5 cm of 5% borated polyethylene, 2.5 cm of aluminum, and another 5 cm of 5% borated polyethylene. The upper part of the can is pure 5% borated polyethylene. It has a compressive strength of 800 psi and can easily support any of the above scatterer materials in the given geometry [Technical Data Sheet, 1984].

4. The MORSE Monte Carlo Transport Code and DABL 69 Library

Description of the Code

The Multigroup Oak Ridge Stochastic Experiment code (MORSE) is a multipurpose neutron and gamma-ray transport Monte carlo code. It features the ability to treat neutron or photon transport or a coupled neutron and secondary gamma-ray transport problem; to solve forward or adjoint problems; to incorporate multigroup cross sections; to solve three-dimensional combinatorial geometries; to solve time dependence for shielding and criticality problems; and to provide numerous variance reduction techniques. Anisotropic scattering for group to group transfer can be modeled by up to a P₁₆ Legendre Polynomial expansion of the angular distribution. MORSE reads cross section data in the DTF-IV or ANISN and DOT format [Cramer, 1985:1-20].

The Defense Applications Broad-group Library (DABL69) was used for this project. It consists of 69 energy groups (46 neutron groups and 23 photon groups) therefore given the acronym DABL69. The DABL69 library is based on the VITAMIN-E multigroup data (which is based on ENDF/B-V files) and more current updates. The DABL69 energy groups and weighting functions were selected to give the most accuracy in most defense related applications. Three weighting functions are used to collapse the cross sections into the

broad-group cross sections to give accuracy in deep penetration problems in air and ferrous materials. Also one of the weighting functions used incorporates a 14.07 MeV fusion peak overlaid on a $1/E$ slowing-down spectrum for neutrons, which is ideal for this analysis. A P_5 Legendre expansion capability exists for group to group scattering matrix for all materials. [Ingersoll et. al., 1989:14-15,20].

Only several of the various available features of MORSE and the DABL69 library were used. For variance reduction, absorption suppression, Russian rouletting in geometries contributing least to the target area, and splitting in geometries contributing most to the target area was used. The anisotropic scattering distribution was modeled by a P_3 Legendre expansion of the angular distribution from the DABL69 cross section library. Studies suggest that a P_3 expansion is sufficient for most applications [Profio, 1979:151-152].

The User Written Routines

The MORSE main program calls upon many subroutines to carry out specific instructions. The main program itself just allocates common blocks, calls subroutines, and ends the program. Standard subroutines included in MORSE perform common tasks applicable to any application. The user can

also generate problem specific subroutines. The subroutines used were generated by others working on typical problems. They are discussed in further detail and presented with the source code in Appendix A.

5. Design Model

Input Geometry Descriptions

The actual geometries used in MORSE to model the target chamber and the test cassette differed slightly from the design geometry. Only one run with the 288 beamlet holes in place was done. The rest of the runs were modified with a correction factor to account for the beamlet holes. The three shock absorbing supports for the shadow shield and the target inserter were not modeled. Since photons that scatter directly behind the shadow shield contribute least to the dose at the test area, the modeling of the target inserter should not be necessary. The wire thin polyethylene shock absorbers should not contribute much dose to the test area.

Source: The Input Spectrum

X Rays

The warm part of the x-ray spectrum of the ICF pellet was modeled using a 6, 8, and 10 keV blackbody spectrum. X rays below 10 keV are not modeled because the DABL69 cross section library does not contain them, therefore the cold x-ray spectrum of the ICF pellet was not modeled. The cold x

rays were assumed to be absorbed in the scatterer, the shadow shield, the can walls or the debris shield.

The number of source photons for the warm x rays is necessary to compute the x-ray dose, dose rates, and energy fluences from the MORSE output. First, integrate Planck's equation (from 10 keV to infinity) of a blackbody emitter for photon number intensity versus photon energy as shown:

$$\int_{10}^{\infty} N(E) dE = \int \frac{2\pi E^2}{c^2 h^3} \left(\frac{1}{(\exp(\frac{E}{kT}) - 1)} \right) dE$$

where c = the speed of light; $2.9979 \times 10^8 \frac{m}{s}$

h = Planck's constant; $4.1357 \times 10^{-18} \text{ keV s}$

kT = the spectrum temperature; 6, 8, or 10 keV

Then, divide by the total energy intensity, I , as shown:

$$I = \sigma T^4$$

where σ = Stefan-Boltzmann constant; $5.670 \times 10^{-8} \frac{J}{m^2 K^4 s}$

T = the temperature in kelvins

The above procedure will yield the source photons per joule for 6, 8, and 10-keV blackbody spectrum.

The MORSE code requires relative inputs for the warm x-ray source spectrum. MORSE uses these relative inputs to create a normalized source spectrum. Integrating the number of photons in each energy group and dividing by the total number of photons gives the contributing fraction of photons for that energy group which MORSE uses to model the warm x-ray source. The fractional inputs need not be modified because of the exclusion of the 0-10 keV photons; MORSE will normalize the source inputs. The calculated values appear in Table 1.

Table 1: Source Photon Spectrum Fractions and Total Source Photons

Photon Energy Group Range	6-keV Blackbody	8-keV Blackbody	10-keV Blackbody
150-300 keV	0	0	0.00003
100-150 keV	0.00001	0.00028	0.00227
70-100 keV	0.00057	0.00605	0.02236
45-70 keV	0.01628	0.06111	0.12039
30-45 keV	0.08713	0.16519	0.21364
20-30 keV	0.19353	0.23339	0.23110
10-20 keV	0.38082	0.32361	0.26298
0-10 keV ^a	0.32166	0.21036	0.14722
Total source photons/MJ	2.608×10^{20}	2.349×10^{20}	1.968×10^{20}

^aEven though this range of photons was not used, the values are shown here provide the reader with the fraction of photons not used.

Neutrons

The source neutrons were modeled using an instantaneous monoenergetic 14.1 MeV neutrons characteristically produced in D-T fusion. Calculating the number of source neutrons per MJ produced in the ICF pellet is necessary to determine the total dose, dose rates, and energy fluences at the test area. A value of 3.547×10^{17} neutrons per MJ of neutron yield was used.

Materials

The MORSE code uses macroscopic cross sections to determine where and when an interaction occurs. The XCHECKER module uses atom number densities of various materials to mix cross-section data in the DABL69 library for input into a MORSE run. The number densities must be expressed in atoms per barn-cm instead of atoms per cm^3 . Appendix E lists the number densities used to model the various materials and the references.

Detector Response Functions

Because the output of the MORSE code is in fluence per source particle (particles per cm^2 per source particle), the user must input detector response functions for the code to provide meaningful results. The detector response functions

for dose due to ionization in silicon are in the DABL69 library. The use of kerma factors assumes that the kinetic energy released in the material (silicon detector) is ultimately absorbed. Messenger and Ash offer a succinct explanation and discussion on kerma factors and their uses [Messenger and Ash, 1986:373-375]. The energy fluence in J/cm^2 is computed by multiplying the fluence by the average energy (in joules) for each energy group. The detector response function values are listed in Appendix F for photons and Appendix G for neutrons.

6. Results and Discussion

Organization

The section will present and discuss the predicted radiation results from the MORSE code and other engineering concerns of the test cassette. First, a summary table is presented showing how the materials compared for an 8 keV warm x-ray temperature without apertures modeled. Then, detailed results for the solid and cryogenic scattering material, results of varying the warm x-ray temperature of the D-T pellet, results of modeling the laser and diagnostic apertures, and results in changing the geometry configuration to achieve increased pulse width are presented. Finally, a comparison between these results and current warm x-ray simulators is made.

The best results were obtained for the lithium hydride scatterers. Enriched lithium hydride performed exceptionally well; it produced at least three times more x-ray dose than any other scattering material configuration. The comparison of dose values is for a 20 MJ D-T ICF pellet with an 8 keV warm x-ray temperature without apertures modeled and a detector distance 2.5 m from the source. The results are summarized in Table 2.

Table 2. Comparison of Dose and Dose Rate Values for Different X-Ray Scattering Materials in the Nova Upgrade for a 20 MJ D-T ICF Pellet. These results do not take apertures into account. Detector distance is 2.5 m from the source.

Material Configuration	Dose (Gy)			X-Ray Dose Rate(Gy/s)
	gamma ray	neutron	x ray	
Lithium Hydride	15.8	27.4	1380	4.92E+11
Lithium Hydride encased in Kapton	30.7	28.7	465	2.99E+11
Polyethylene	32.5	21.0	298	1.68E+11
Hydrogen	29.8	28.9	302	1.99E+11
Helium	30.7	28.7	286	1.73E+11
Methane	30.7	28.7	203	1.21E+11

Solid Scattering Material

Lithium Hydride

Lithium hydride enriched to 96.5% performed the best of all the materials. In the test cassette configuration, the dose from an 8 kev blackbody emitter for a detector distance of 2.5 m was 6.89 ± 0.10 kGy/MJ (689 krad(Si)/MJ) of ICF pellet warm x-ray energy yield. The peak dose rate was

2.46×10^{12} Gy/MJ. Neutron and gamma ray doses were 1.96 ± 0.04 Gy/MJ and 1.13 ± 0.04 Gy/MJ of ICF pellet neutron energy yield, respectively. For a 20 MJ pellet with a 8 keV blackbody spectrum and 1% warm x-ray yield, greater than 97% of the total dose is warm x-ray dose with only 1.9% and 1.1% of the dose due to neutrons and gamma rays, respectively. Also, the peak dose rate was 4.92×10^{11} Gy/s (4.92×10^{13} rads(Si)/s) and the energy fluence on the test area was 0.126 cal/cm^2 . Table 3 shows the dose values for the lithium hydride scatterer and the percent contributions toward the total dose.

Table 3. Dose Values for Lithium Hydride Scatterer in the Nova Upgrade Chamber without Apertures Modeled. Results are for an 8 keV warm x-ray temperature at a point detector 2.5 m from the source.

	Output Response (Gy/ source particle)	Fractional Standard Deviation of the Output Response (See below)	Dose per MJ yield (Gy/MJ) (See below)	Dose @ 20 MJ for 1% x-ray yield (Gy)	% of Total Dose for 20 MJ ICF D-T fusion pellet with warm x-ray yield of:			
					1%	2%	3%	5%
Gamma	3.19×10^{-18}	0.033	1.13 ^a	15.8	1.1	0.6	0.4	0.2
Neutron	5.52×10^{-18}	0.007	1.96 ^a	27.4	1.9	1.0	0.7	0.4
X-Ray	2.93×10^{-17}	0.014	6890 ^b	1380	97.0	98.5	99.0	99.4

^aGamma ray and neutron dose per MJ of neutron yield of the ICF source. ^bX ray does per MJ of warm x-ray yield of the ICF source.

Lithium hydride encased in Kapton did not perform as well. For the 8 keV spectrum, encased lithium hydride

produced a 2.33 ± 0.03 kGy/MJ x-ray dose, a 2.05 ± 0.01 Gy/MJ gamma ray dose, and a 2.19 ± 0.07 Gy/MJ neutron dose. The peak dose rate was 1.50×10^{12} Gy/s. This amounts to a 66% reduction in x-ray dose, 5% increase in neutron dose and a 94% increase in gamma ray dose. For a 1% warm x-ray yield, the peak dose rate was 2.99×10^{10} Gy/s with a pulse width of 1.5 ns. Table 4 lists the dose results over a range of warm x-ray parameters the percent contributions toward the total dose.

Table 4. Values for Lithium Hydride Scatterer Encased in 10 mils of Kapton. Results are for an 8 keV warm x-ray temperature at a point detector 2.5 m from the source.

	Output Response (Gy/source particle)	Fractional Standard Deviation of the Output Response (See below)	Dose per MJ of yield (Gy/MJ) (See below)	Dose @ 20 MJ for 1% x-ray yield (Gy)	% of Total Dose for 20 MJ ICF D-T fusion pellet with warm x-ray yield of:			
					1%	2%	3%	5%
Gamma	6.18E-17	0.033	2.19 ^a	30.7	5.9	3.1	2.1	1.3
Neutron	5.78E-18	0.007	2.05 ^a	28.7	5.5	2.9	2.0	1.2
X-Ray	9.90E-17	0.014	2330 ^b	465	88.7	94.0	95.9	97.5

^aGamma ray and neutron dose per MJ of neutron yield of the ICF source. ^bX ray does per MJ of warm x-ray yield of the ICF source.

Polyethylene

Polyethylene did not perform quite as well as lithium hydride. For the 8 keV spectrum, polyethylene yielded 1.49 ± 0.38 kGy/MJ warm x-ray dose, 2.32 ± 0.05 Gy/MJ gamma ray dose, and 1.50 ± 0.04 Gy/MJ neutron dose. For 1% warm x-ray yield, the peak dose rate was 1.68×10^{11} Gy/s with a pulse width of 1/2 ns. Although the polyethylene did not perform as well as lithium hydride, the warm x-ray dose and dose rate are significant enough for warm x-ray tests and the neutron dose is below DNA's 10% desired neutron dose level.

Table 5 lists the results over a range of warm x-ray parameters.

Table 5. Dose Values for a Polyethylene Scatterer. Results are for an 8 keV warm x-ray temperature at a point detector 2.5 m from the source.

	Output Response (Gy/source particle)	Fractional Standard Deviation of the Output Response	Dose per MJ of yield (Gy/MJ)	Dose @ 20 MJ for 1% x-ray yield (Gy)	% of Total Dose for 20 MJ ICF D-T fusion pellet with warm x-ray yield of:			
					1%	2%	3%	5%
Gamma	6.54E-18	0.019	2.32 ^a	32.49	9.3	5.0	3.4	2.1
Neutron	4.23E-18	0.026	1.50 ^a	21.04	6.0	3.2	2.2	1.4
X-Ray	6.33E-18	0.025	1490 ^b	297.5	84.8	91.8	94.3	96.5

^a Gamma ray and neutron dose per MJ of neutron yield of the ICF source.

^b X ray does per MJ of warm x-ray yield of the ICF source.

Cryogenic Scattering Material

Hydrogen

Liquid hydrogen encased in 10 mils of Kapton performed the best of the cryogenic material, but not as quite as well as lithium hydride. For the 8 keV spectrum, liquid hydrogen yielded 1.51 ± 0.07 kGy/MJ x-ray dose, 2.13 ± 0.05 Gy/MJ gamma ray dose, and 2.06 ± 0.08 Gy/MJ neutron dose. For a 1% warm x-ray yield, the peak dose rate was 2.0×10^{11} Gy/s with a pulse width of 1.5 ns. Table 6 lists the results of liquid hydrogen over a range of warm x-ray parameters.

Table 6. Values for a Liquid Hydrogen Scatterer Encased in 10 mils of Kapton. Results are for an 8 keV warm x-ray temperature at a point detector 2.5 m from the source.

	Output Response (Gy/ source particle)	Fractional Standard Deviation of the Output Response	Dose per MJ of yield (Gy/MJ)	Dose @ 20 MJ for 1% x-ray yield (Gy)	% of Total Dose for 20 MJ ICF D-T fusion pellet with warm x-ray yield of:			
					1%	2%	3%	5%
Gamma	6.01E-18	0.025	2.13 ^a	29.8	8.3	4.5	3.1	1.9
Neutron	5.81E-18	0.044	2.06 ^a	28.9	8.0	4.4	3.0	1.8
X-Ray	6.44E-18	0.045	1510 ^b	302.4	83.7	91.2	93.9	96.3

^aGamma ray and neutron dose per MJ of neutron yield of the ICF source. ^bX ray does per MJ of warm x-ray yield of the ICF source.

After the ICF pellet ignition, the Kapton casing may burst. Assuming all of the cold x-rays and debris deposits all of its energy into the liquid hydrogen, only 28% of hydrogen becomes vapor. If all of the hydrogen were to heat

up to room temperature (290 K), the vapor pressure would be 0.82 atmospheres. Since the original pressure inside the target chamber was a vacuum, the additional pressure would help relieve some of the buckling stress from the outside atmosphere.

Helium

Liquid helium did not perform quite as well as liquid hydrogen. For the 8 keV spectrum, helium produced a 1.43 ± 0.05 kGy/MJ x-ray dose, a 2.19 ± 0.07 Gy/MJ gamma ray dose, and a 2.05 ± 0.01 Gy/MJ neutron dose. For a 1% warm x-ray yield, the x-ray dose was 286 ± 9 Gy and the peak dose rate was 1.73×10^{11} Gy/s with a pulse width of 1.5 ns. Table 7 lists the results for liquid helium over a range of warm x-ray parameters.

Table 7. Values for a Liquid Helium Scatterer Encased in 10 mils of Kapton. Results are for an 8 keV warm x-ray temperature at a point detector 2.5 m from the source.

	Output Response (Gy/source particle)	Fractional Standard Deviation of the Output Response	Dose per MJ of yield (Gy/MJ)	Dose @ 20 MJ for 1% x-ray yield (Gy)	% of Total Dose for 20 MJ ICF D-T fusion pellet with warm x-ray yield of:			
					1%	2%	3%	5%
Gamma	6.18E-18	0.033	2.19 ^a	30.7	8.9	4.9	3.4	2.1
Neutron	5.78E-18	0.007	2.05 ^a	28.7	8.3	4.6	3.1	1.9
X-Ray	6.08E-17	0.031	1430 ^b	286	82.8	90.6	93.5	96.0

^aGamma ray and neutron dose per MJ of neutron yield of the ICF source. ^bX ray does per MJ of warm x-ray yield of the ICF source.

As with liquid hydrogen, the broken casing may release helium inside the target chamber. Assuming all of the cold x-rays and debris deposits all of its energy into the liquid helium, 100% of the helium becomes vapor. If all of the helium were to heat up to room temperature (290 K), the vapor pressure would be 0.36 atmospheres. Again, the additional pressure would help relieve some of the buckling stress from the outside atmosphere.

Methane

Liquid methane did not perform quite as well as liquid hydrogen or helium. For the 8 keV spectrum, liquid methane produced a 1.01 ± 0.03 kGy/MJ warm x-ray dose, a 2.19 ± 0.07 Gy/MJ gamma ray dose, and a 2.05 ± 0.01 Gy/MJ neutron dose. For a 1% warm x-ray yield, the peak dose rate was 1.68×10^{11} with a pulse width of 1.5 ns. Table 8 lists the results for liquid methane over a range of warm x-ray parameters.

Table 8. Values for a Liquid Methane Scatterer Encased in 10 mils of Kapton. Results are for an 8 keV warm x-ray temperature at a point detector 2.5 m from the source.

	Output Response (Gy/source particle)	Fractional Standard Deviation of the Output Response	Dose per MJ of yield (Gy/MJ)	Dose @ 20 MJ for 1% x-ray yield (Gy)	% of Total Dose for 20 MJ ICF D-T fusion pellet with warm x-ray yield of:			
					1%	2%	3%	5%
Gamma	6.18E-18	0.033	2.19 ^a	30.7	11.7	6.6	4.6	2.9
Neutron	5.78E-18	0.007	2.05 ^a	28.7	11.0	6.2	4.3	2.7
X-Ray	4.30E-17	0.027	1010 ^b	202	77.3	87.2	91.1	94.5

^aGamma ray and neutron dose per MJ of neutron yield of the ICF source. ^bX ray does per MJ of warm x-ray yield of the ICF source.

Effect of Warm X-Ray Spectrum Temperature

As the temperature spectrum of the warm x rays vary, it is not predictable as to whether a change in this temperature will cause an increase or decrease in the x-ray dose. For a cooler spectrum, an increased number of cooler

x rays will contribute more to the x-ray dose if they make it to the test area. The scatterer may absorb too many of these cooler x rays thus reducing the warm x-ray fluence at the test area. Table 9 shows that the polyethylene and liquid methane reduce the x-ray dose for a cooler warm x-ray temperature. For the hotter x-ray temperature, the dose always decreased.

Table 9. Comparison of Dose in Silicon from Various Warm X-ray Blackbody Temperatures.

	Response (Gy/source x ray)			Dose (Gy/MJ of x-ray energy)			Change from 8 keV Baseline	
	6 keV	8 keV	10 keV	6 keV	8 keV	10 keV	6 keV	10 keV
Lithium Hydride	3.04E-17	2.93E-17	2.88E-17	7930	6890	5660	+15.0%	-17.9%
LiH in Kapton	1.01E-17	9.90E-18	9.21E-18	2640	2330	1810	+13.6%	-22.0%
Liquid Hydrogen	6.55E-18	6.44E-18	5.97E-18	1710	1510	1180	+13.0%	-22.3%
Liquid Helium	5.79E-18	6.08E-18	5.70E-18	1510	1430	1120	+5.70%	-21.5%
Liquid Methane	3.76E-18	4.30E-18	4.44E-18	980	1010	874	-2.93%	-13.5%
Poly-ethylene	5.51E-18	6.33E-18	6.56E-18	1440.	1490.	1290.	-3.35%	-13.3%

Effect of the Capture Gamma Rays

Over 50% of the dose attributed to gamma rays could be included as part of the x-ray dose. Figure 5 below shows that about half of the gamma ray fluence is in the warm x-ray region. Figure 6 shows the response function for

photons and neutrons. It can easily be seen that the majority of the gamma ray dose is in the warm x-ray region.

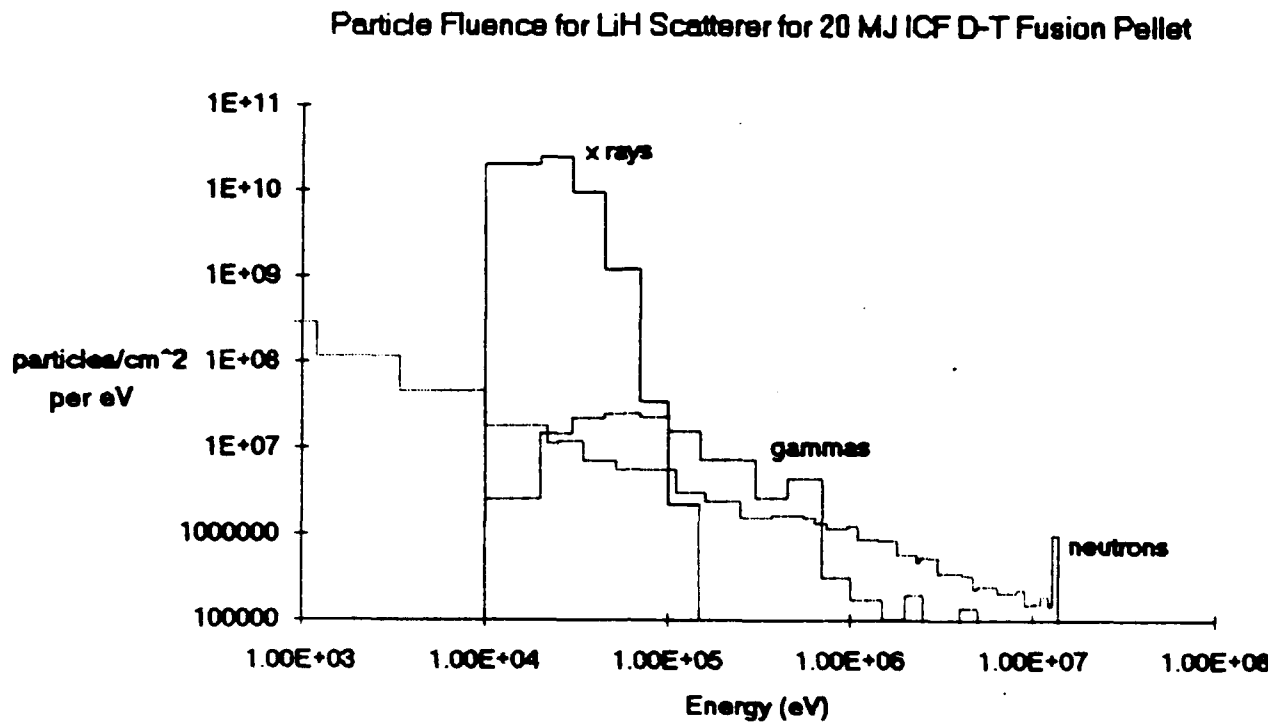


Figure 5. Particle Fluence for a Lithium Hydride Scatterer.

Response Function in Silicon for Particle Fluence

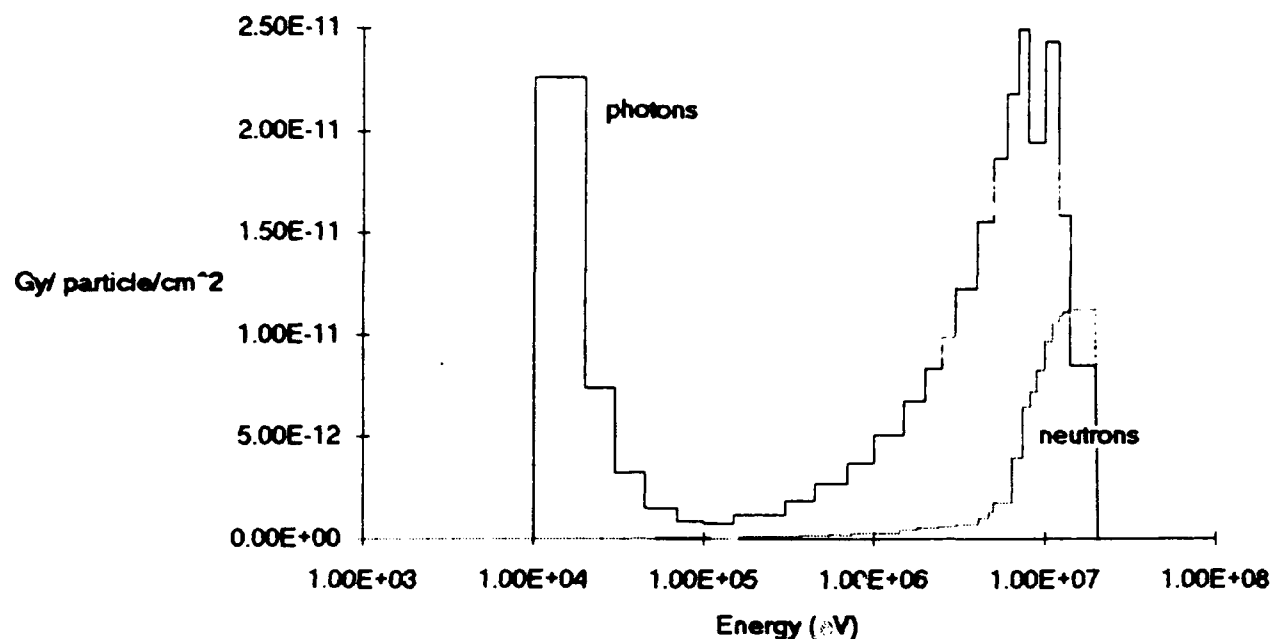


Figure 6. Silicon Response Functions for Photons and Neutrons.

Although, the gamma rays may add to the x-ray dose, they will contribute little to the dose rate. While the x-ray dose is delivered over nanoseconds of time, the gamma ray dose is spread over a period of shakes. Figure 7 shows the gamma ray dose rate versus time.

Neutron and Gamma Dose Rate for LiH Scatterer for 20 MJ ICF D-T Fusion Pellet

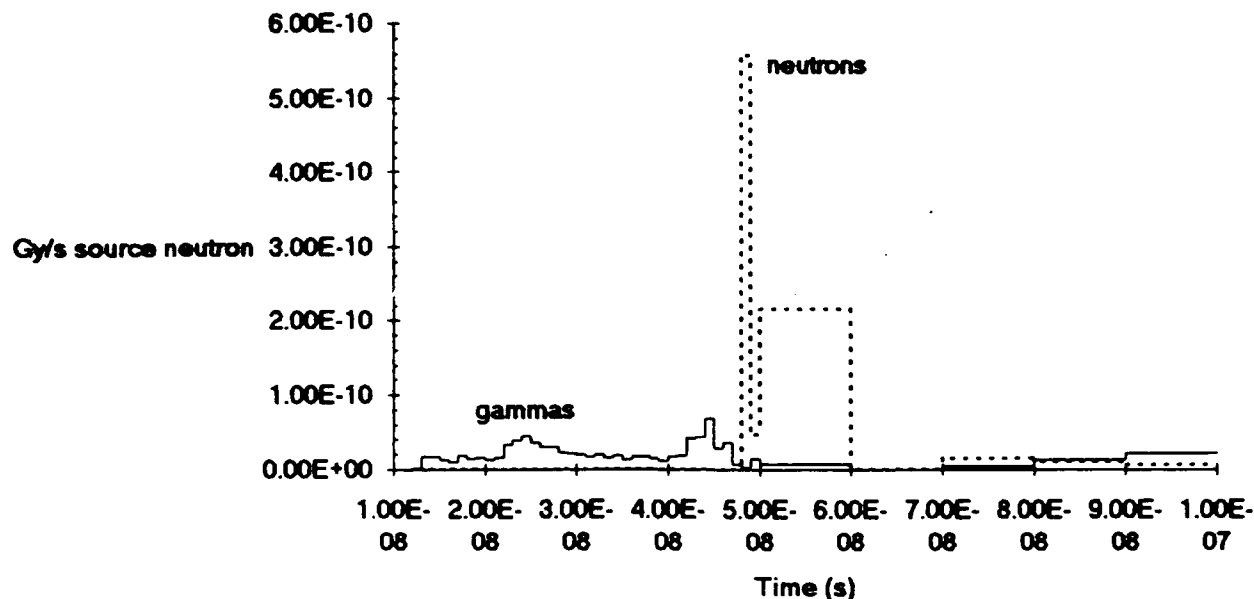


Figure 7. Neutron and Gamma Ray Dose Rates for Lithium Hydride Scatterer.

The Effect of Apertures

A simple geometry was used to gauge the effect of the laser and diagnostic apertures on the test area. Modeling all of the apertures is a very time consuming process which requires a large volume of input and days to run using the MORSE code on the VAX system. To predict the effect of the apertures, the geometry was modeled with a 10 cm thick hemispherical lithium hydride scatterer on top of a cassette can with shadow shield, debris shield, and all 288 apertures in place. The shadow shield and debris shield were the same as in previous geometries, but the cassette can encased 2.5 cm of Aluminum 5083 with 5 cm of 5% borated polyethylene outside of it and 2.5 cm inside of it.

Introducing the apertures into the test cassette had some predictable results. When the 288 laser apertures are modeled in the lithium hydride scatterer, the apertures remove approximately 8% of the solid angle surrounding the ICF pellet. For this 8% reduction in the solid angle, the neutron dose decreased $18 \pm 1\%$ and the gamma ray dose decreased $21 \pm 2\%$. Since more of the source neutrons (which contribute the most to the neutron dose) escape directly out of the test cassette, there are less fast neutrons in the test cassette to contribute to the neutron dose. Since high energy neutrons create high energy gamma rays, this reduced amount of fast neutrons create less capture gamma rays. So, the gamma ray dose is reduced more so than the neutron dose.

The x-ray reduction was not so predictable. One would initially think that at least an 8% reduction of the x-ray dose should occur. Only a $6.8 \pm 0.2\%$ reduction occurred. The x rays that scatter toward the top of the scatterer contribute less to the dose at the test area at the bottom; because the x-ray scattering is near isotropic, the dose contribution per steradian is less. Likewise, the loss of these x rays that would have scattered toward the top of the scatterer also contribute less to the reduction of dose at the test area.

The actual reduction in dose will vary with geometry and material. Materials that produce a different number or

different energy of capture gamma rays will effect the gamma ray reduction by the presence of the apertures. Scatterers that are of different thickness toward the top of the scatterer than at the sides will effect the reduction of all three doses. But the actual reduction in solid angle for all the apertures will be 10% allowing for diagnostic equipment in addition to the beamlets. For comparison purposes, assuming a proportional relationship between radiation loss and percent apertures, x-ray doses were reduced 8.5%, gamma ray dose 26%, and neutron dose 22%. Accounting for the reduction for the apertures, the dose and dose rate values for the scattering materials are summarized in Table 10.

Table 10. Comparison of Dose and Dose Rate Values for Different X-Ray Scattering Materials in the Nova Upgrade for a 20 MJ D-T ICF Pellet with Apertures Modeled. A 1% warm x-ray yield is assumed. These results take apertures into account. Detector distance is 2.5 m from the source.

Material Configuration	Dose (Gy)			X-Ray Dose Rate (Gy/s)
	gamma ray	neutron	x ray	
Lithium Hydride	11.7	21.4	1260	4.50E+11
Lithium Hydride encased in Kapton	22.7	22.4	425	2.74E+11
Polyethylene	24.0	16.4	272	1.54E+11
Hydrogen	22.0	22.5	277	1.82E+11
Helium	22.7	22.4	262	1.58E+11
Methane	22.7	22.4	186	1.11E+11

Effect of Geometry Changes on Pulse Width

Since some radiation effects depend on the pulse width (defined at full width at half maximum) of the dose over time, maximizing this value may be of importance for some tests. To increase the pulse width, the time over which the dose is deposited must be lengthened. This can be accomplished in two ways. First, the geometry of the scatterer can be changed such that the x rays reach the scatterer over a longer period of time and thus arrive at the test area over a longer time. Second, changing the density of the scatterer such that some of the x rays scatter deeper into the material thus arriving at the target over a greater period of time.

Currently, the most promising is the first method of changing the geometry. By simply raising the scatterer from 25 cm to 55 cm from the source, Figure 8 illustrates a five fold increase in the pulse width. In the Nova Upgrade target chamber, there is not sufficient space to stretch this into the 10's of nanoseconds required by some tests.

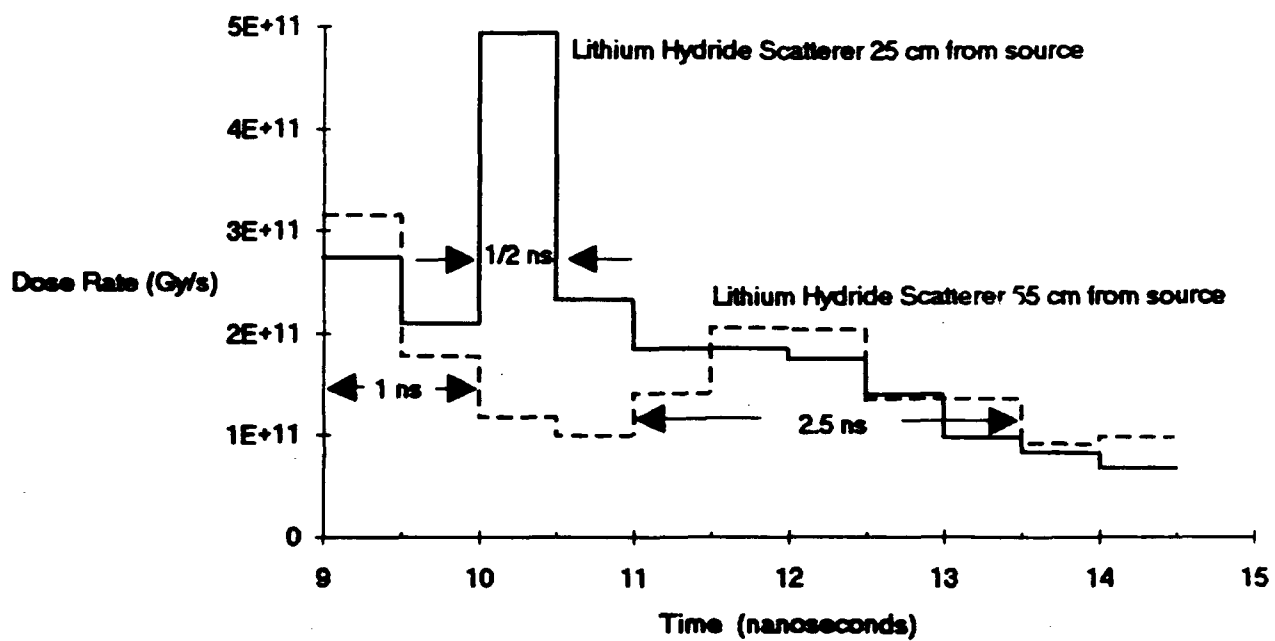


Figure 8. Comparison of Varying Geometry to Lengthen Pulse Width

Comparison with Current Simulators

To get an appreciation of what the results mean, a comparison of the predicted results against current NWET simulators with the ability to test in the warm x-ray region reveals clear advantages. For the comparison purposes, the results for a lithium hydride scatterer with an assumed ICF pellet output of 8 keV and 1% warm x-ray yield is used. A 8.5% reduction for laser and diagnostic apertures was assumed. Table 11 compares the most commonly used features in NWET simulators.

Table 11. Comparison of Current NWET Simulators and Predicted Radiation Environment in Nova Upgrade

	Dose in krad (Si)	Dose Rate in rads(Si) per sec	Area (cm ²)	Fluence (cal/cm ²)	Uniformity Dose _{min} / Dose _{max}	Pulse Width (ns)	Peak Energy (keV)	Spectral End Point (keV)
Nova Upgrade	126	4.5×10^{13}	13270	1.2×10^{-1}	90%	1	25	150
MBS(PI) ^a	0.3	5×10^9	1000	1.5×10^{-4}	85%	60	100	250
MBS ^b	0.35	5.7×10^9	3000	2×10^{-4}	83%	31-38	150	200
DECADE ^c (future)	20	5×10^{11}	10000	N/A	N/A	N/A	N/A	1500

^a[Rix et al, 1988:47-54], ^b[Schneider et al, 1988:55-63], ^c[Pressley, 1991], N/A signifies not available.

The Nova Upgrade with the lithium hydride scatterer has the advantage in all categories except pulse width. Three orders of magnitude increase in dose and four orders of

magnitude increase in dose rate over present day simulators is apparent. If the assumed ICF pellet x-ray yield was increased to 2% of the dose, dose rate, and energy fluence results become even more dramatic. Two other notable advantages are the uniformity in the delivery of the dose and dose rate over the test area and the large test area itself. The next generation simulator, DECADE, is predicted to perform similarly to the liquid methane scatterer, which was the least favorable material used.

7. Summary, Recommendations and Conclusions

Summary

The ICF environment in the Nova Upgrade can be modified using a test cassette to provide a warm x-ray test environment suitable for DNA's present day needs. The most promising scattering material is 95.6% enriched lithium hydride. With the use of the MORSE Monte Carlo code and the DABL69 Broad-group cross section library, a warm x-ray dose of 6.30 ± 0.09 kGy/MJ of warm x-ray yield with less than 1% of the dose due to neutrons is predicted. For a nominal 20 MJ yield and 1% warm x-ray yield, the predicted warm x-ray dose is 1.26 ± 0.02 kGy, and the peak dose rate is 1.5×10^{11} Gy/s. This dose and dose rate easily surpass the present day warm x-ray simulator capability by three orders of magnitude and at the same time provides an order of magnitude increase in exposure area for testing. Other materials examined contributed significant warm x-ray fluences suitable for NWET. All of the neutron doses were below the desired limit of 10% after the reduction for apertures is applied.

Recommendations for Future Work

The optimization of the shadow shield needs further examination. The majority of the neutron dose is from

neutrons which pass through the shadow shield. The present configuration has 4 mean free paths thickness for 14.1 MeV neutrons. Since the shadow shield is already as close as allowable to the source, any increase in the thickness of the shadow shield will be added to the bottom thus decreasing the x-ray fluence to the test area. An initial start may be to increase the tungsten thickness, since it has a higher attenuation coefficient than the borated polyethylene.

The DABL69 library contains photon cross section information only down to 10 keV. So, the low energy photons that could contribute significantly to the warm x-ray dose are not modeled. The use of a library containing photon cross section data below 10 keV should give a more precise prediction. This may significantly increase dose and dose rate since the kerma is much larger for photons of that energy.

An analysis of the effect of activation after the ICF pellet shot on the test area is needed. The intense fluence of high energy neutrons will activate materials in the target chamber. Approximately 4 hours are needed to evacuate the radioactive gases from the target chamber. During these 4 hours the activation products will contribute a dose to the test area. The dose effects from this exposure needs to be looked into.

Conclusions

The Nova Upgrade does have the potential to provide a better warm x-ray test environment for hardened electronics than current NWET simulators. Its dose, dose rate, and exposure area created by the insertion of a test cassette are greater than what currently exists today or planned in the next generation simulator. Enriched lithium hydride is the most promising scattering material for the warm x-ray test environment.

Bibliography

American Society for Metals. *Metals Handbook* (Ninth Edition). Volume 2, *Properties and Selection: Nonferrous Alloys and Pure Metals*. Metals Park, Ohio: ASM, 1978.

Compressed Gas Association. *Handbook of Compressed Gases* (Third Edition). New York: Van Nostrand Reinhold, 1990.

Cramer, S. N. *Applications Guide to the MORSE Monte Carlo Code*. ORNL/TM-9355. Oak Ridge, Tennessee: Oak Ridge National Laboratory, August 1985.

Daniels, Carole A. *Polymers; Structure & Properties*. Lancaster, Pennsylvania: Technomic Publishing Company, 1989.

Emmitt, M. B. *The MORSE Monte Carlo Radiation Transport Code System*. ORNL-4972/R2. Oak Ridge, Tennessee: Oak Ridge National Laboratory, July 1984.

GE Nuclear Operations. *Nuclides and Isotopes* (Fourteenth Edition). Revised by F. William Walker et al. San Jose, California: General Electric Company, 1989.

Glasstone, Samuel and Philip J. Dolan. *The Effects of Nuclear Weapons* (Third Edition). Washington, D.C.: Government Printing Office, 1977.

Gullickson, R. L., Electromagnetic Applications Division, Radiation Sciences Directorate, Defense Nuclear Agency. Handout distributed in conference on Nova Upgrade for Nuclear Weapons Effects Testing. Washington, D.C., 8 July 1991.

Inertial Confinement Fusion. Lawrence Livermore National Laboratory. Livermore, California: Government Printing Office, July 1989.

Ingersoll, D. T. et al. *DABL69: A Broad-Group Neutron/Photon Cross-Section Library for Defense Nuclear*

Applications. ORNL/TM-10568. Oak Ridge, Tennessee: Oak Ridge National Laboratory, 1989.

Kennedy, Tom, Test Directorate, Defense Nuclear Agency.
Address to members in conference on Nova Upgrade for Nuclear Weapons Effects Testing. Washington, D.C., 20 August 1991.

Krane, Kenneth S. Introductory Nuclear Physics. New York: John Wiley & Sons, Inc., 1988.

Mark, Herman F. et al. Encyclopedia of Polymer Science and Technology; Plastics, Resins, Rubbers, and Fibers, Volume 11. New York: Interscience Publishers, 1964.

Merritt, Frederick S. Standard Handbook for Civil Engineers (Third Edition). New York: McGraw-Hill Book Co., 1983.

Messenger, George C. and Milton S. Ash. The Effects of Radiation on Electronic Systems. New York: Van Nostrand Reinhold Co., 1986.

Pike, R. A. "Polyimides for Water Soluble Precursors," Polyimides; Synthesis, Characterization, and Applications, Volume 1, edited by K. L. Mittal. New York: Plenum Press, 1982.

Pressley, Leonard, Jr., Group Leader, Simulator Operations, Electromagnetic Applications Division, Defense Nuclear Agency. Presentation to members in conference on Nova Upgrade for Nuclear Weapons Effects Testing. Washington, D.C., 8 July 1991.

Profio, A. Edward. Radiation Shielding and Dosimetry. New York: John Wiley & Sons, 1979.

Shielding and Foils. Product Catalog 20. Reactor Experiments, Inc., San Carlos, California, 1982.

Seaman, L. et al. Continuing Assessment of Debris Generation from a Megajoule Inertial Confinement Fusion

Experimental Facility. Purchase Order No. B063696.
Menlo Park, California: SRI International, May 1989.

Shrinet, V. et al. "Effect of Neutron & Proton Irradiation on some Properties of Kapton," *Polyimides; Synthesis, Characterization, and Applications*, Volume 1, edited by K. L. Mittal. New York: Plenum Press, 1982.

Technical Data Sheet, Polyethylene-Base Shielding. Bulletin S-87N. Reactor Experiments, Inc., San Carlos, California, April 1984.

Tobin, Michael J., Project Leader, Nova Upgrade Target Area. Personal and telephone interviews. Lawrence Livermore National Laboratory, Livermore, California, September through November 1991.

Tobin, Michael J. et al. *Target Area for Nova Upgrade: Containing Ignition and Beyond.* Contract W-7405-ENG-48. Draft of paper to be submitted to IEEE conference on 23-27 September 1991. Livermore, California and Los Alamos, New Mexico: Lawrence Livermore and Los Alamos National Laboratories, September 1991.

Weast, Robert C., Editor. *CRC Handbook of Chemistry & Physics (1st Student Edition).* Boca Raton, Florida: CRC Press Inc., 1988.

Appendix A: User Written Routines for MORSE

The MORSE Monte Carlo Code operates through a main program through a series of multiple subroutines. The main program itself merely allocates memory, reads inputs, outputs file names, and terminates execution. The other various subroutines are written separate so that the user can modify them to suit his needs or use default versions of the subroutines. In a typical Monte Carlo calculation, a particle is born from a source. The particle is given a position, direction, speed, and time (if time dependent). The path length to the next collision is given in mean free paths. The particle is then tracked through the various geometries until the collision or escape occurs. Boundary crossings are tallied and the program determines if a new particle is created. The MORSE code will be described using these functions.

Subroutine BANKR tracks significant events such as particle birth at source, particle production, collisions, boundary crossings, and escape. BANKR calls the flux estimators such as RELCOL, SDATA, and SGAM. RELCOL is used to calculate flux estimations to the point detectors after each collision. SDATA provides data to RELCOL on uncollided flux estimations from the source. SGAM provides similar data to RELCOL but on secondary particles generated by collisions. Subroutine BDRXY is called by banker whenever a

boundary crossing begins. GTMED assignr. the different media in the combinatorial geometry to different zones for rouletting, splitting, and other actions. STRUN does nothing in this application, but exists for user input for problems involving time fissioning. It is executed at the beginning of each batch. Function DIREC would be used if the user wanted to implement exponential transform for path stretching.

FORTRAN Source Code

Main Routine

```
C      LMF.FOR
C*****
C*      This version determines uncollided fluence and others.      *
C*      a collision-density estimator is used to determine      *
C*      fluence and is called for each collision. This version      *
C*      includes SDATA for source neutrons, SGAM for neutron-      *
C*      generated gammas, and RELCOL for others.      *
C*****
C * * THIS IS THE MAIN ROUTINE * * * * * * * * * * * * * * * * * * *
C * * D. Beller July 89. 1 detector in LMF for X-ray effects
C * * THE FOLLOWING CARD DETERMINES THE SIZE ALLOWED FOR BLANK COMMON *
c * * The value of NLFT below should be set to one less than this size
COMMON NC(100001)
C * * (REGION SIZE NEEDED IS ABOUT 150K + 4*(SIZE OF BLANK COMMON IN WO
C * * NOTE - THE ORDER OF COMMONS IN THIS ROUTINE IS IMPORTANT AND MUST
C * * POND TO THE ORDER USED IN DUMP ROUTINES SUCH AS HELP, XSCHLP, AN
C * *
C * * LABELLED COMMONS FOR WALK ROUTINES    * * * * * * * * * * * *
COMMON /APOLLO/ AGSTRT,DDF,DEADWT(26),ITOUT,ITIN
COMMON /FISBNK/ MFISTP
COMMON /NUTRON/ NAME
C * *
C * * LABELLED COMMONS FOR CROSS-SECTION ROUTINES * * * * * * * * * *
COMMON /LOCSIG/ ISCCOG
COMMON /MEANS/ NM
COMMON /MOMENT/ NMOM
COMMON /QAL/ Q
COMMON /RESULT/ POINT
C * *
C * * LABELLED COMMONS FOR GEOMETRY INTERFACE ROUTINES * * * * * * * *
COMMON /GEOMC/ XTWO
COMMON /NORMAL/ UNORM
C * *
C * * LABELLED COMMONS FOR USER ROUTINES * * * * * * * * * * * *
COMMON /PDET/ ND
COMMON /USER/ AGST
C * *
C * * COMMON /DUMMY/ WILL NOT BE FOUND ELSEWHERE IN THE PROGRAM * * * *
COMMON /DUMMY/ DUM
C * *
CHARACTER*40, NAM1
CHARACTER*40, NAM2
TYPE *,'
TYPE *,***** MORSE Code, LMF X-Ray Effects Problem *****
TYPE *,'=====> WARNING !!! <====='
TYPE *,'ABORT if mixed x-secs are not assigned to FOR010'
```

```
      TYPE *,'
      TYPE *,'ENTER NAME OF INPUT FILE'
      ACCEPT 100, NAM1
100    FORMAT(A40)
      TYPE *,'ENTER NAME OF OUTPUT FILE'
      ACCEPT 200, NAM2
200    FORMAT (A40)
      OPEN(UNIT=1,NAME=NAM1,TYPE='OLD')
      OPEN(UNIT=2,NAME=NAM2,TYPE='NEW')
      ITOUT = 2
      ITIN = 1
      NLFT=100000
      CALL MORSE(NLFT)
      TYPE 300, NAM2
300    FORMAT(X,'OUTPUT FILE IS ',A40)
      STOP
      END
```

Subroutine GTMED

```
SUBROUTINE GTMED(MDGEOM,MDXSEC)
C FOR SETTING CROSS SECTIONS IN THE INPUT DATA FILE FOR MORSE
c IF(MDGEOM.GT.0 .AND. MDGEOM.LT.1000) MDXSEC = MDGEOM
MDXSEC = MDGEOM
RETURN
END
```

Function DIREC

```
FUNCTION DIREC
COMMON /NUTRON/ NAME,NAMEX,IG,IGO,NMED,MEDOLD,NREG,U,V,W,UOLD,VOLD
1 ,WOLD,X,Y,Z,XOLD,YOLD,ZOLD,WATE,OLDWT,WTBC,BLZNT,BLZON,AGE,OLDAGE
c for pathlength stretching toward the detectors (in the +y direction)
DATA XD,YD,ZD/0.,400.,0/
DIST = SQRT((XD-X)**2+(YD-Y)**2+(ZD-Z)**2)
DIREC = (U*(XD-X)+V*(YD-Y)+W*(ZD-Z))/DIST
C
RETURN
END
```

Subroutine BANKR

```
SUBROUTINE BANKR(NBNKID)
C DO NOT CALL EUCLID FROM BANKR(7)
COMMON /APOLLO/ AGSTRT,DDF,DEADWT(5),ETA,ETATH,ETAUSD,UINP,VINP,
1 WINP,WTSTRT,XSTRT,YSTRT,ZSTRT,TCUT,XTRA(10),
2 10,11,MEDIA,IADJM,ISBIAS,ISOUR,ITERS,ITIME,ITSTR,LOCWTS,LOCFWL,
3 LOCEPR,LOCNSC,LOCFSN,MAXGP,MAXTIM,MEDALB,MGPREG,MXREG,NALB,
4 NDEAD(5),NEWNM,NGEOM,NGPQT1,NGPQT2,NGPQT3,NGPQTG,NGPQTN,NITS,
5 NKCALC,NKILL,NLAST,NMEM,NMGP,NMOST,NMTG,NOLEAK,NORMF,NPAST,
6 NPSCL(13),NQUIT,NSIGL,NSOUR,NSPLT,NSTRT,NXTRA(10)
COMMON /NUTRON/ NAME,NAMEX,IG,IGO,NMED,MEDOLD,NREG,U,V,W,UOLD,VOLD
1 ,WOLD,X,Y,Z,XOLD,YOLD,ZOLD,WATE,OLDWT,WTBC,BLZNT,BLZON,AGE,OLDAGE
NBNK = NBNKID
IF (NBNK) 100,100,140
100 NBNK = NBNK + 5
GO TO (104,103,102,101),NBNK
101 CALL STRUN
C CALL HELP(4HSTRU,1,1,1,1)
RETURN
102 NBAT = NITS - ITERS
NSAVE = NMEM
CALL STBTCH(NBAT)
C NBAT IS THE BATCH NO. LESS ONE
RETURN
103 CALL NBATCH(NSAVE)
C NSAVE IS THE NO. OF PARTICLES STARTED IN THE LAST BATCH
RETURN
104 CALL NRUN(NITS,NQUIT)
C NITS IS THE NO. OF BATCHES COMPLETED IN THE RUN JUST COMPLETED
C NQUIT .GT. 1 IF MORE RUNS REMAIN
C .EQ. 1 IF THE LAST SCHEDULED RUN HAS BEEN COMPLETED
C IS THE NEGATIVE OF THE NO. OF COMPLETE RUNS, WHEN AN
C EXECUTION TIME KILL OCCURS
RETURN
140 GO TO (1,2,3,4,5,6,7,8,9,10,11,12,13),NBNK
C NBNKID COLL TYPE BANKR CALL NBNKID COLL TYPE BANKR CALL
C 1 SOURCE YES (MSOUR) 2 SPLIT NO (TESTW)
C 3 FISSION YES (FPROB) 4 GAMGEN YES (GSTORE)
C 5 REAL COLL YES (MORSE) 6 ALBEDO YES (MORSE)
C 7 BDRYX YES (NXTCOL) 8 ESCAPE YES (NXTCOL)
C 9 E-CUT NO (MORSE) 10 TIME KILL NO (MORSE)
C 11 R R KILL NO (TESTW) 12 R R SURV NO (TESTW)
C 13 GAMLOST NO (GSTORE)

1 CALL SDATA
2 RETURN
3 RETURN
4 Call SGAM
Return
5 CALL RELCOL
```

```
    RETURN
6  RETURN
7  RETURN
8  RETURN
9  RETURN
10 RETURN
11 RETURN
12 RETURN
13 RETURN
END
```

Subroutine SDATA

```
SUBROUTINE SDATA                               SDATA 10
c
c this version D. Beller, 12 July 1989, for an isotropic point
c source located at (X,Y,Z) and for point detectors 1 to ND located
c at (XD,YD,ZD). Cos of angle is not stored!!!
c
COMMON /USER/ AGSTRT,WTSTRT,XSTRT,YSTRT,ZSTRT,DFF,EBOTN,EBOTG,      SDATA 20
1 TCUT,I0,11,IADJM,NGPQT1,NGPQT2,NGPQT3,NGPQTG,NGPQTN,NITS,NLAST,   SDATA 21
2 NLEFT,NMGP,NMTG,NSTRT                           SDATA 22
COMMON /PDET/ ND,NNE,NE,NT,NA,NRESP,NEX,NEXND,NEND,NDNR,NTNR,NTNE,SDATA 30
1 NANE,NTNDNR,NTNEND,NANEND,LOCRSP,LOCXD,LOCIB,LOCCT,LOCJ,LOCN      SDATA 31
2 LOCSD,LOCQE,LOCQT,LOCQTE,LOCQAE,LMAX,EFIRST,EGTOP                  SDATA 32
COMMON /NUTRON/ NAME,NAMEX,IG,IGO,NMED,MEDOLD,NREG,U,V,W,UOLD,VOLDS DATA 40
1 ,WOLD,X,Y,Z,XOLD,YOLD,ZOLD,WATE,OLDWT,WTBC,BLZNT,BLZON,AGE,OLDAGES DATA 41
COMMON EN(1)                                     SDATA 50
ENEST = 1.0
DO 5 I=1,ND                                     SDATA 80
ID = LOCXD + I
XE = EN(ID)
YE = EN(ID + ND)
ZE = EN(ID + 2*ND)
A = XE - X
B = YE - Y
C = ZE - Z
SD2 = A*A + B*B + C*C
SD = SQRT(SD2)
c diagnostic
if(name.eq.1) type *, 'detector', I,'source-detector distance = ', SD
c comment this out if sdata is working well
TA = SD/EN(NMTG + IG) + AGE
MARK = 1
CALL EUCLID(MARK,X,Y,Z,XE,YE,ZE,SD,IG,ARG,0,NMED,BLZNT,NREG)
IF (ARG.LT.-32) GO TO 5
CON = WATE*EXP(ARG)/12.56637/SD2/ENEST
c      if (con.ge.0) goto 555
c      type *, 'consdata =',con
555  CALL FLUXST(I,IG,CON,TA,1.0,1)
5     Continue
C * * SWITCH = -1 -- STORE IN ARRAY UD ONLY
C * *           1 -- Store in array UD and others          SDAT 150
RETURN                                         SDAT 160
END                                            SDAT 170
```

Subroutine SGAM

```

SUBROUTINE SGAM                               SGAM  10
C   Added for LMF problem 6 Feb 90 by D. Beller    * * * *
C   THIS VERSION IS FOR POINT DETECTORS LOCATED AT (XD,YD,ZD)    * * * *
C   AND FOR AN ISOTROPIC POINT SOURCE    * * * *
C
C   COMMON /USER/ AGSTRT,WTSTR,XTSTR,YSTR,ZSTR,DFF,EBOTN,EBOTG,    SGAM  60
1  TCUT,IO,I1,IADJM,NGPQT1,NGPQT2,NGPQT3,NGPQTG,NGPQTN,NITS,NLAST,    SGAM  61
2  NLEFT,NMGP,NMTG,NSTRT                           SGAM  62
COMMON /PDET/ ND,NNE,NE,NT,NA,NRESP,NEX,NEXND,NEND,NDNR,NTNR,NTNE,SGAM  70
1  NANE,NTNDNR,NTNEND,NANEND,LOCRSP,LOCXD,LOCIB,LOCCO,LOCCT,LOCUD,    SGAM  71
2  LOCSD,LOCQE,LOCQT,LOCQTE,LOCQAE,LMAX,EFIRST,EGTOP               SGAM  72
COMMON /NUTRON/ NAME,NAMEX,IG,IGO,NMED,MEDOLD,NREG,U,V,W,UOLD,VOLD,SGAM  80
1 ,WOLD,X,Y,Z,XOLD,YOLD,ZOLD,WATE,OLDWT,WTBC,BLZNT,BLZON,AGE,OLDAGESGAM  81
COMMON EN(1)                                     SGAM  90
DO 5 I=1,ND                                      SGAM 100
ID = LOCXD + I                                    SGAM 110
XE = EN(ID)                                       SGAM 120
ID = ID + ND                                      SGAM 130
YE = EN(ID)                                       SGAM 140
ID = ID + ND                                      SGAM 150
ZE = EN(ID)                                       SGAM 160
A=X -XE                                         SGAM 170
B=Y -YE                                         SGAM 180
C=Z -ZE                                         SGAM 190
SD2=A*A+B*B+C*C                                 SGAM 200
DS = SQRT(SD2)                                     SGAM 210
TA = DS/EN(NMTG+IG)+AGE                          SGAM 220
C * * * COS      DEPENDS ON THE ANGLE OF INTEREST    * * * *
MARK = 1                                           SGAM 260
MEDIUM=NMED                                       SGAM 270
CALL EUCLID(MARK,X,Y,Z,XE,YE,ZE,DS,IG,ARG,0 ,MEDIUM,BLZNT,NREG)    SGAM 280
if (arg.lt.-64) goto 5
CON = WATE *EXP(ARG)/12.56637/SD2                SGAM 290
C * * * SWITCH = 1 -- STORE IN ALL RELEVANT ARRAYS    SGAM 300
C next two lines for current info
C   COS=C/DS                                         SGAM 250
J   CALL FLUXST(I,IG,CON,TA,COS,1)                  SGAM 310
CALL FLUXST(I,IG,CON,TA, 0 ,1)
5   CONTINUE                                         SGAM 320
RETURN                                            SGAM 330
END                                              SGAM 340

```

Subroutine RELCOL

```

SUBROUTINE RELCOL                               RELCO 10
C
C THIS VERSION IS FOR POINT DETECTORS LOCATED AT (XD,YD,ZD)      RELCO 20
C
C
COMMON /USER/ AGSTRT,WTSTRT,XSTRT,YSTRT,ZSTRT,DFF,EBOTN,EBOTG,      RELCO 30
1 TCUT,I0,I1,IADJM,NGPQT1,NGPQT2,NGPQT3,NGPQTG,NGPQTN,NITS,NLAST,   RELCO 40
2 NLEFT,NMGP,NMTG,NSTRT                         RELCO 50
COMMON /PDET/ ND,NNE,NE,NT,NA,NRESP,NEX,NEXND,NEND,NDNR,NTNR,NTNE,RELCO 60
1 NANE,NTNDNR,NTNEND,NANEND,LOCRSP,LOCXD,LOCIB,LOCCO,LOCT,LOCUD,    RELCO 61
2 LOCSD,LOCQE,LOCQT,LOCQTE,LOCQAE,LMAX,EFIRST,EGTOP                RELCO 62
COMMON /NUTRON/ NAME,NAMEX,IG,IGO,NMED,MEDOLD,NREG,U,V,W,UOLD,VOLDRELCO 70
1 ,WOLD,X,Y,Z,XOLD,YOLD,ZOLD,WATE,OLDWT,WTBC,BLZNT,BLZON,AGE,OLDAGERELCO 71
COMMON BL(1)                                     RELCO 80
DIMENSION NL(1)                                 RELCO 90
EQUIVALENCE (BL(1),NL(1))                      RELC 100
DATA NEST /2/, FNEST /2./

C above is RELC 110
C NEST + FNEST ARE THE NO. OF ESTIMATES TO BE MADE TO EACH DETECTOR RELC 130
C * * * ISTAT MUST BE EQUAL TO 1.                                * * * *
C * * * NEX MUST BE AT LEAST 1.                                * * * *
C * * * NEXND MUST BE AT LEAST 1.                                * * * *
DO 30 I=1,ND                                         RELC 160
IA=LOCKXD+I                                         RELC 170
XE = BL(IA)                                         RELC 180
YE = BL(IA+ND)                                      RELC 190
ZE = BL(IA+2*ND)                                     RELC 200
A = XE - X                                         RELC 210
B = YE - Y                                         RELC 220
C = ZE - Z                                         RELC 230
SD2=A*A+B*B+C*C                                     RELC 240
DS=SQRT (SD2)                                       RELC 250
C * * * COS DEPENDS ON THE ANGLE OF INTEREST          * * * *
COS=C/DS                                           RELC 270
THETA = (A*UOLD + B*VOLD + C*WOLD)/DS             RELC 280
IGOLD = IGO                                         RELC 290
IGQ = NGPQT3                                       RELC 300

IF (IGO.LE.NGPQT1) IGQ=NGPQT1                     RELC 310
IA = LOCRSP + NRESP*NMTG + 1                      RELC 320
CALL PTHETA(NMED,IGOLD,IGQ,THETA,BL(IA),NMTG)     RELC 330
NES = 0                                              RELC 340
PSUM = 0.                                            RELC 350
IA = IA - 1                                         RELC 360
DO 5 IL=IGOLD,IGQ                                    RELC 370
5 PSUM = PSUM + (BL(IA+IL))                        RELC 380
C samples from a normalized distr without negative Legendre coeffs removed
10 R = FLTRNF(0) * PSUM                            RELC 390
DO 15 IL=IGOLD,IGQ                                  RELC 400
if (bl(ia+il).lt.0) goto 15

```

```

if (r .lt. 0) goto 15
IF (R - (BL(IA+IL))) 20,20,15
15 R = R - (BL(IA+IL))
IL = IGQ
20 MARK=1
AGED = AGE + DS/BL(NMTG+IL)
MEDIUM=NMED
CALL EUCLID(MARK,X,Y,Z,XE,YE,ZE,DS,IL,ARG,0,MEDIUM,BLZNT,NREG)
IF (ARG.LT.-64.) GO TO 25
C*****BEWARE THIS VERSION WILL NOT WORK IF ENERGY BIASING IS USED
CON = WATE*EXP (ARG)*SIGN (PSUM,BL(IA+IL))/SD2/FNEST
C * * * couldn't handle 1e-40
IF (CON.LT.1.0E-36) GO TO 25
c      type *, 'con=', con, ' group = ', il, ' wate = ', wate,
c      l' exp = ', exp(arg), 'bl(ia+il) = ', bl(ia+il), 'distance = ', ds
CALL FLUXST (I,IL,CON,AGED,COS,0)
25 NES = NES + 1
INN=LOCXD+6*ND+1
NL(INN)=NL(INN)+1
IF (NES-NEST) 10,30,30
30 CONTINUE
RETURN
END

```

```

TRC  4  0.0000 0  0.0000 0 -0.3400+2  0.0000 0  0.0000+0 -0.0900+2
      110.50-1  139.75-1
SPH  5  0.0000 0  0.0000 0  0.0000 0  4.0000+2  0.0000 0  0.0000 0
SPH  6  0.0000 0  0.0000 0  0.0000 0  4.0500+2  0.0000 0  0.0000 0
SPH  7  0.0000 0  0.0000 0  0.0000 0  4.2500+2  0.0000 0  0.0000 0
SPH  8  0.0000 0  0.0000 0  0.0000 0  5.0000+2  0.0000 0  0.0000 0
SPH  9  0.0000 0  0.0000 0  0.0000 0  10.000+2  0.0000 0  0.0000 0
RCC 10  0     0     -30.000+0 0     0     -3.629 +2
      .7500+2
RCC 11  0     0     -2.0000+2 0     0     -1.929 +2
      0.7000+2
RCC 12  0     0     -30.000+0 0     0     -3.629 +2
      0.6750+2
RCC 13  0     0     -30.000+0 0     0     -3.629 +2
      0.6500+2
RCC 14  0     0     -1.490+2 0     0     -0.025 +0
      0.5500+2
RCC 15  0     0     -30.000+0 0     0     -1.300 +2
      0.6500+2
RCC 16  0     0     -30.00+0 0     0     -1.300 +2
      0.5500+2
SPH 17  0.0000 0  0.0000 0 -30.000 0  55.025  00.000 0  00.000 0
END
ivd   +5    -1    -100R  +2    -30R  +13   -150R  +16   -3
      -14
CON   +1    -17   -100R  +17   -2    -15
pgB   +3    -4
pgL   +4
kop   +14
Cn1   +10   -11   -12
Cn2   +11   -12
Cn3   +12   -13
Cn4   +15   -16
1WL   +6    -5
ply   +7    -6
VOD   +9    -7
END
      1    2    2    2    2    2    2    2    1    1    1    1    1
      1000 8    6    4    3    4    5    4    8    5    2    0
46 N, 23 GAMMA (P3) for NOVA Upgrade w/Scatterer Sphere & Can Ellipse
      46   46   23   23   69   72   4    8    21   32   4    2    1    3
      0    0    0    0    0    0    0   -10   0    0    0
SAMBO ANALYSIS INPUT DATA for Nova Upgrade
      4   43   66   -52   0    6   12   8
      0.0   00.0   -150.0
      0.0   00.0   -250.0
      0.0   00.0   -350.0
      0.0   55.0   -350.0

```

RESULTS of Nova Upgrade calculation -- Neutron-Gamma simulation

Gamma Ionization in Silicon {Gy(Si)/source particle (Gammas Dose)}

0.0	0.0	0.0	0.0	0.0	0.0	0.0
0.0	0.0	0.0	0.0	0.0	0.0	0.0

0.0	0.0	0.0	0.0	0.0	0.0	0.0
0.0	0.0	0.0	0.0	0.0	0.0	0.0
0.0	0.0	0.0	0.0	0.0	0.0	0.0
0.0	0.0	0.0	0.0	0.0	0.0	0.0
0.0	0.0	0.0	0.0	8.5045E-12	1.5823E-11	2.4318E-11
1.9441E-11	2.485E-11	2.175E-11	1.862E-11	1.545E-11	1.222E-11	9.803E-12
8.284E-12	6.718E-12	5.074E-12	3.681E-12	2.657E-12	1.841E-12	1.120E-12
7.454E-13	8.359E-13	1.447E-12	3.211E-12	7.3881E-12	2.2600E-11	
Neutron Ionization in Silicon {Gy(Si)/source particle (Neutrons Dose)}						
1.4136E-111	1.1867E-111	1.1380E-111	1.1213E-111	1.1108E-111	1.0931E-111	1.0560E-111
9.6552E-128	2.573E-128	1.1892E-126	4.233E-123	9.406E-121	7.265E-121	3.041E-121
9.9411E-136	4.401E-135	8.343E-135	9.385E-135	0.306E-134	0.888E-132	2.068E-133
2.2945E-132	6.028E-132	5.167E-132	1.4625E-131	9.371E-131	2.283E-131	0.185E-131
1.1136E-135	3.753E-157	6.044E-154	0.843E-152	5.145E-151	9.299E-151	3.058E-151
5.7105E-161	7.532E-166	5.553E-172	7.522E-173	1.906E-171	5.852E-175	8.717E-18
2.5149E-182	7.854E-187	5.570E-188	8.589E-180	0.0000E+000	0.0000E+000	0.0000E+000
0.0000E+000	0.0000E+000	0.0000E+000	0.0000E+000	0.0000E+000	0.0000E+000	0.0000E+000
0.0000E+000	0.0000E+000	0.0000E+000	0.0000E+000	0.0000E+000	0.0000E+000	0.0000E+000
0.0000E+000	0.0000E+000	0.0000E+000	0.0000E+000	0.0000E+000	0.0000E+000	0.0000E+000
Gamma Fluence (gammas/cm ² /source particle)						
0.0	0.0	0.0	0.0	0.0	0.0	0.0
0.0	0.0	0.0	0.0	0.0	0.0	0.0
0.0	0.0	0.0	0.0	0.0	0.0	0.0
0.0	0.0	0.0	0.0	0.0	0.0	0.0
0.0	0.0	0.0	0.0	0.0	0.0	0.0
0.0	0.0	0.0	0.0	0.0	0.0	0.0
0.0	0.0	0.0	0.0	1.0	1.0	1.0
1.0	1.0	1.0	1.0	1.0	1.0	1.0
1.0	1.0	1.0	1.0	1.0	1.0	1.0
1.0	1.0	1.0	1.0	1.0	1.0	1.0
Neutron Fluence (neutrons/cm ² /source neutron)						
1.0	1.0	1.0	1.0	1.0	1.0	1.0
1.0	1.0	1.0	1.0	1.0	1.0	1.0
1.0	1.0	1.0	1.0	1.0	1.0	1.0
1.0	1.0	1.0	1.0	1.0	1.0	1.0
1.0	1.0	1.0	1.0	1.0	1.0	1.0
1.0	1.0	1.0	1.0	1.0	1.0	1.0
1.0	1.0	1.0	1.0	0.0	0.0	0.0
0.0	0.0	0.0	0.0	0.0	0.0	0.0
0.0	0.0	0.0	0.0	0.0	0.0	0.0
0.0	0.0	0.0	0.0	0.0	0.0	0.0
Gammas (joules/cm ⁻² /source particle)						
0.0	0.0	0.0	0.0	0.0	0.0	0.0
0.0	0.0	0.0	0.0	0.0	0.0	0.0
0.0	0.0	0.0	0.0	0.0	0.0	0.0
0.0	0.0	0.0	0.0	0.0	0.0	0.0
0.0	0.0	0.0	0.0	0.0	0.0	0.0
0.0	0.0	0.0	0.0	0.0	0.0	0.0
0.0	0.0	0.0	0.0	2.7234E-12	2.0826E-12	1.7622E-12
1.4418E-12	1.2015E-12	1.0413E-12	8.8110E-13	7.2090E-13	5.6070E-13	4.4055E-13
3.6045E-13	2.8035E-13	2.0025E-13	1.3617E-13	9.2115E-14	6.0075E-14	3.6045E-14
2.0025E-14	1.3617E-14	9.2115E-15	6.0075E-15	4.0050E-15	2.4030E-15	

Neutrons (joules/cm⁻²/source particle)

2.9237-12 2.5472-12 2.3309-12 2.2428-12 2.1307-12 2.0025-12 1.8663-12
1.6901-12 1.5219-12 1.3777-12 1.2496-12 1.1054-12 9.1314-13 7.7697-13
7.0488-13 5.6871-13 4.3254-13 3.7647-13 3.2841-13 2.5814-13 2.0207-13
1.6514-13 1.4278-13 1.2524-13 1.1070-13 9.5261-14 7.3598-14 4.9347-14
3.2620-14 2.1627-14 1.2976-14 6.9132-15 4.7505-15 3.7547-15 2.5532-15
1.0733-15 3.6846-16 1.4258-16 6.8514-17 3.0066-17 1.0333-17 3.2040-18
1.1294-18 3.3642-19 1.2127-19 3.3162-20 0.0000E+0 0.0000E+0 0.0000E+0
0.0000E+0 0.0000E+0 0.0000E+0 0.0000E+0 0.0000E+0 0.0000E+0
0.0000E+0 0.0000E+0 0.0000E+0 0.0000E+0 0.0000E+0 0.0000E+0
0.0000E+0 0.0000E+0 0.0000E+0 0.0000E+0 0.0000E+0 0.0000E+0
{particles/cm²/eV/source neutron}

4	5	6	7	8	9	10	11	12	13	14	15	16	17
18	19	20	21	22	23	24	25	26	27	28	29	30	31
32	33	34	35	36	37	38	39	40	41	42	43	44	45
46	47	48	49	50	51	52	53	54	55	56	57	58	59
60	61	62	63	64	65	66	67	68	69				

([1-2 Gy(Si) 3-4 part/cm² 5-6 J/cm²] /sec/Source Particle)

(particles/cm²/eV/sec/source particle)

0.7e-8	0.8e-8	0.9e-8	1.0e-8	1.1e-8	1.2e-8	1.3e-8
1.4e-8	1.5e-8	1.6e-8	1.7e-8	1.8e-8	1.9e-8	2.0e-8
2.1e-8	2.2e-8	2.3e-8	2.4e-8	2.5e-8	2.6e-8	2.7e-8
2.8e-8	2.9e-8	3.0e-8	3.1e-8	3.2e-8	3.3e-8	3.4e-8
3.5e-8	3.6e-8	3.7e-8	3.8e-8	3.9e-8	4.0e-8	4.1e-8
4.2e-8	4.3e-8	4.4e-8	4.5e-8	4.6e-8	4.7e-8	4.8e-8
4.9e-8	5.0e-8	7.0e-8	6.0e-8	8.0e-8	9.0e-8	1.0e-7
1.0e-5	1.0e-4	1.0e-3				

||||||| Nova Upgrade Neutron-Gamma Effects Simulation 91 |||||

Appendix C: Example of MORSE Data Output File

Problem to determine X-Ray effects in Nova Upgrade (8 keV) Ellipse
TODAY IS 12-13-91

NSTRT	NMOST	NITS	NCOUT	NGPOTN	NGPOTG	NMGF	NMTG	NCOLTP	IADJM	MAXIM	MEDIA	MEDALB
1000	4000	5	1	0	10	10	10	0	0	300.00	8	0

ISOUR	NGPFS	ISBIAS	WTSTART	EBOTN	EBOTG	TCUT	VELTH
0	10	0	1.0000E+00	0.0000E+00	1.0000E+04	1.0000E-03	2.2000E+05

XSTART	YSTRT	ZSTART	AGSTART	UINP	VINP	WINP
0.000L+00	0.000E+00	0.000E+00	0.000L+00	0.000000	0.000000	0.000000

SOURCE DATA

GROUP	UNNORMALIZED	NORMALIZED
	FRACTION	FRACTION
1	0.0000E+00	0.000000
2	0.0000E+00	0.000000
3	0.0000E+00	0.000000
4	1.4819E-06	0.000001
5	3.5820E-04	0.000358
6	7.6594E-03	0.007659
7	7.7390E-02	0.077391
8	2.0919E-01	0.209192
9	2.9557E-01	0.295573
10	4.0982E-01	0.409824
TOTAL	9.9999L-01	

GROUP PARAMETERS, GROUP NUMBERS GREATER THAN 0 CORRESPOND TO SECONDARY PARTICLES

GROUP	UPPER EDGE (EV)	VELOCITY (CM/SEC)
1	1.0000E+05	2.9979E+10
2	7.0000E+05	2.9979E+10
3	4.5000E+05	2.9979E+10
4	3.0000E+05	2.9979E+10
5	1.5000E+05	2.9979E+10
6	1.0000L+05	2.9979E+10
7	7.0000E+04	2.9979E+10
8	4.5000E+04	2.9979E+10
9	3.0000E+04	2.9979E+10
10	2.0000E+04	2.9979E+10

INITIAL RANDOM NUMBER = 45 FA231A

NSPLT= 1 NKILL= 1 NPAST= 0 NOLEAK= 0 IEIAS= 0 MXREG= 3 MAXGP= 10

WEIGHT STANDARDS FOR SPLITTING AND RUSSIAN ROULETTE AND PATHLENGTH STRETCHING PARAMETERS

NGP1 NGC NGP2 NRG1 NRG NRG2 WTHIH1 WTLOW1 WTAVE1 XNI

1	1	10	1	1	1	1.0000E+00	1.0000E-01	1.0000E+00	0.0000E+00
1	1	10	2	1	3	1.0000E+00	1.0000E-05	4.0000E+00	0.0000E+00

NSOUR= 0 MFISTP= 0 NKCALC= 0 NORMF= 0

COMBINATORIAL GEOMETRY Nova Upgrade

MOP1 = 0 IDBG = 0

BODY DATA

ELL	1	0.00000000+00	0.00000000+00	-0.21540000+03	0.00000000+00	0.00000000+00	0.15540000+03	3
		0.40000000+23						
SPH	2	0.00000000+00	0.00000000+00	-0.30000000+02	0.55000000+02	0.00000000+00	0.00000000+00	12
TRC	3	0.00000000+00	0.00000000+00	-0.25000000+02	0.00000000+00	0.00000000+00	-0.18000000+02	20
		0.81250000+01	0.13975000+02					
TRC	4	0.00000000+00	0.00000000+00	-0.34000000+02	0.00000000+00	0.00000000+00	-0.90000000+01	30
		0.11050000+02	0.13975000+02					
SPH	5	0.00000000+00	0.00000000+00	0.00000000+00	0.40000000+03	0.00000000+00	0.00000000+00	40
SPH	6	0.00000000+00	0.00000000+00	0.00000000+00	0.40500000+03	0.00000000+00	0.00000000+00	48
SPH	7	0.00000000+00	0.00000000+00	0.00000000+00	0.42500000+03	0.00000000+00	0.00000000+00	56
SPH	8	0.00000000+00	0.00000000+00	0.00000000+00	0.50000000+03	0.00000000+00	0.00000000+00	64
SPH	9	0.00000000+00	0.00000000+00	0.00000000+00	0.10000000+04	0.00000000+00	0.00000000+00	72
RCC	10	0.00000000+00	0.00000000+00	-0.30000000+02	0.00000000+00	0.00000000+00	-0.36290000+03	80
		0.75000000+02						
RCC	11	0.00000000+00	0.00000000+00	-0.20000000+03	0.00000000+00	0.00000000+00	-0.19290000+03	89
		0.70000000+02						
RCC	12	0.00000000+00	0.00000000+00	-0.30000000+02	0.00000000+00	0.00000000+00	-0.36290000+03	98
		0.67500000+02						
RCC	13	0.00000000+00	0.00000000+00	-0.30000000+02	0.00000000+00	0.00000000+00	-0.36290000+03	107
		0.65000000+02						
RCC	14	0.00000000+00	0.00000000+00	-0.14900000+03	0.00000000+00	0.00000000+00	-0.25000000-01	116
		0.55000000+02						
RCC	15	0.00000000+00	0.00000000+00	-0.30000000+02	0.00000000+00	0.00000000+00	-0.13000000+03	125
		0.65000000+02						
RCC	16	0.00000000+00	0.00000000+00	-0.30000000+02	0.00000000+00	0.00000000+00	-0.13000000+03	134
		0.55000000+02						
END	17	0.00000000+00	0.00000000+00	0.00000000+00	0.00000000+00	0.00000000+00	0.00000000+00	143

NUMBER OF BODIES 16

LENGTH OF FPD-ARRAY 148

INPUT ZONE DATA

ivd	0	5	-1	-100R	2	-30R	13	-150R	16	-3	Z	1
	0	-14	0	0	0	0	0	0	0	0	Z	5
CON	0	1	-2	-10	0	0	0	0	0	0	Z	5
pqB	0	3	-4	0	0	0	0	0	0	0	Z	6
pql	0	4	0	0	0	0	0	0	0	0	Z	7
kap	0	14	0	0	0	0	0	0	0	0	Z	8
Cn1	0	10	-11	-12	0	0	0	0	0	0	Z	9
Cn2	0	11	-12	0	0	0	0	0	0	0	Z	10

Cn3	0	12	-13	0	0	0	0	0	0	0	Z 11
Cn4	0	15	-16	0	0	0	0	0	0	0	Z 12
IWL	0	6	-5	0	0	0	0	0	0	0	Z 13
phy	0	7	-6	0	0	0	0	0	0	0	Z 14
VOD	0	9	-7	0	0	0	0	0	0	0	Z 15
END	0	0	0	0	0	0	0	0	0	0	Z 16
NUMBER OF INPUT ZONES				12							
NUMBER OF CODE ZONES				15							
LENGTH OF INTEGER ARRAY				376							

CODE ZONE	INPUT ZONE	ZONE DATA LOC.	NO. OF BODIES	REGION NO.	MEDIA NO.
1	1	113	3	1	1000
2	1	126	2	1	1000
3	1	135	2	1	1000
4	1	144	3	1	1000
5	2	157	3	2	8
6	3	170	2	1	6
7	4	179	1	1	4
8	5	184	1	2	3
9	6	189	3	2	4
10	7	202	2	2	5
11	8	211	2	2	4
12	9	220	2	2	8
13	10	229	2	1	5
14	11	238	2	1	2
15	12	247	2	1	0

I	KR1(I)	KR2(I)
1	1	4
2	5	5
3	6	6
4	7	7
5	8	8
6	9	9
7	10	10
8	11	11
9	12	12
10	13	13
11	14	14
12	15	15

MORSE REGION IN INPUT ZONE(I) ARRAY MRIZ(I),I=1,12

1 2 1 1 2 2 2 2 2 1 1 1

MORSE MEDIA IN INPUT ZONE(I) ARRAY MMIZ(I),I=1,12

1000 8 6 4 3 4 5 4 8 5 2 0

OPTION 0 WAS USED IN CALCULATING VOLUMES, FOR 2 REGIONS
0-SET VOLUMES = 1, 1-CONCENTRIC SPHERES, 2-SLABS, 3-INPUTVOLUMES.

VOLUMES (CM**3) USED IN COLLISIONS DENSITY AND TRACK LENGTH ESTIMATORS.
REG 1 2
VOLUME 1.0000+00 1.0000+00

NGEOM= 1015, NGLAST= 1830

46 N, 23 GAMMA (P3) for NOVA Upgrade with Scatterer Sphere & Can Ellipse

NUMBER OF PRIMARY GROUPS (NGP) 0
NUMBER OF PRIMARY DOWNSCATTERS (NDS) 0
NUMBER OF SECONDARY GROUPS (NGG) 10
NUMBER OF SECONDARY DOWNSCATTERS (NDSC) 10
NUMBER OF PRIM+SEC GROUPS (INGP) 69
TABLE LENGTH (ITBL) 72
LOC OF WITHIN GROUP (SIG GG) (ISGG) 4
NUMBER OF MEDIA (NMED) 8
NUMBER OF INPUT ELEMENTS (NELEM) 21
NUMBER OF MIXING ENTRIES (NMIX) 37
NUMBER OF COEFFICIENTS (NCOEF) 4
NUMBER OF ANGLES (NSCT) 2
RESTORE COEFF (ISTAT) 1
ADJOINT SWITCH (FROM MORSE) 0

INPUT/OUTPUT OPTIONS

IRDSC (AS READ) 0
ISTR (AS STORE) 0
IFMU (MUS) 0
IMOM (MOMENTS) 0
IPRIN (ANGLES,PROB) 0
IPUN (IMPOSSIBLE COEF) 0
CARD FORMAT (IDTF) 0
INPUT TAPE (IXTAP) -10
MORSEC TAPE (JXTAPE) 0
OGR TAPE (IOGRT) 0
CROSS SECTIONS START AT 1831
LAST LOCATION USED (PERM) 6046

**** THE FOLLOWING VALUES ARE FROM TAPE. ****
Lower 10 X Ray groups (P3) for Nova Upgrade Weapons Effects

NUMBER OF PRIMARY GROUPS (NGP) 10
NUMBER OF PRIMARY DOWNSCATTERS (NDS) 10
NUMBER OF SECONDARY GROUPS (NGG) 0
NUMBER OF SECONDARY DOWNSCATTERS (NDSC) 0
NUMBER OF PRIM+SEC GROUPS (INGP) 69

TABLE LENGTH (ITBL)	72
LOC OF WITHIN GROUP (SIG GG) (ISGG)	4
NUMBER OF MEDIA (NMED)	8
NUMBER OF INPUT ELEMENTS (NELEM)	21
NUMBER OF MIXING ENTRIES (NMIX)	37
NUMBER OF COEFFICIENTS (NCOEF)	4
NUMBER OF ANGLES (NSCT)	2
RESTORE COEFF (ISTAT)	1
ADJOINT SWITCH (FROM MORSE)	0

BANKS START AT 6047
LAST LOCATION USED 54046

SAMBO ANALYSIS INPUT DATA for Nova Upgrade

ND= 4, NNE= 0, NE= 10, NT=-35, NA= 0, NRESP= 3, NEX= 12, NEXNO= 8

DET	X	Y	Z	RAD	T0
1	0.0000E+00	0.0000E+00	-1.5000E+02	1.5000E+02	5.0035E-09
2	0.0000E+00	0.0000E+00	-2.5000E+02	2.5000E+02	8.3392E-09
3	0.0000E+00	0.0000E+00	-3.5000E+02	3.5000E+02	1.1675E-08
4	0.0000E+00	5.5000E+01	-3.5000E+02	3.5430E+02	1.1818E-08

GROUP	RESP(1)	RESP(2)	RESP(3)
1	3.6810E-12	1.0000E+00	1.3617E-13
2	2.6570E-12	1.0000E+00	9.2115E-14
3	1.8410E-12	1.0000E+00	6.0075E-14
4	1.1200E-12	1.0000E+00	3.6045E-14
5	7.4540E-13	1.0000E+00	2.0025E-14
6	8.3590E-13	1.0000E+00	1.3617E-14
7	1.4470E-12	1.0000E+00	9.2115E-15
8	3.2110E-12	1.0000E+00	6.0075E-15
9	7.3881E-12	1.0000E+00	4.0050E-15
10	2.2600E-11	1.0000E+00	2.4030E-15

NUMBER OF PRIMARY ENERGY BINS	0		
TOTAL NUMBER OF ENERGY BINS	10		
LOWER	LOWER		
BIN NO.	LIMIT	ENERGY	DELTA
	GROUP	LIMIT	E
		1.000E+06	
1	1	7.000E+05	3.000E+05
2	2	4.500E+05	2.500E+05
3	3	3.000E+05	1.500E+05
4	4	1.500E+05	1.500E+05
5	5	1.000E+05	5.000E+04
6	6	7.000E+04	3.000E+04
7	7	4.500E+04	2.500E+04
8	8	3.000E+04	1.500E+04
9	9	2.000E+04	1.000E+04

10 10 1.000E+04 1.000E+04

NUMBER OF TIME BINS 35

FOR DETECTOR 1

UPPER LIMITS OF TIME BINS

5.0000E-09	5.5000E-09	6.0000E-09	6.5000E-09	7.0000E-09	7.5000E-09	8.0000E-09
8.5000E-09	9.0000E-09	9.5000E-09	1.0000E-08	1.0500E-08	1.1000E-08	1.1500E-08
1.2000E-08	1.2500E-08	1.3000E-08	1.3500E-08	1.4000E-08	1.4500E-08	1.5000E-08
1.5500E-08	1.6000E-08	1.6500E-08	1.7000E-08	1.7500E-08	1.8000E-08	1.8500E-08
1.9000E-08	2.0000E-08	2.1000E-08	2.2000E-08	2.3000E-08	2.4000E-08	2.5000E-08

FOR DETECTOR 2

UPPER LIMITS OF TIME BINS

5.0000E-09	5.5000E-09	6.0000E-09	6.5000E-09	7.0000E-09	7.5000E-09	8.0000E-09
8.5000E-09	9.0000E-09	9.5000E-09	1.0000E-08	1.0500E-08	1.1000E-08	1.1500E-08
1.2000E-08	1.2500E-08	1.3000E-08	1.3500E-08	1.4000E-08	1.4500E-08	1.5000E-08
1.5500E-08	1.6000E-08	1.6500E-08	1.7000E-08	1.7500E-08	1.8000E-08	1.8500E-08
1.9000E-08	2.0000E-08	2.1000E-08	2.2000E-08	2.3000E-08	2.4000E-08	2.5000E-08

FOR DETECTOR 3

UPPER LIMITS OF TIME BINS

5.0000E-09	5.5000E-09	6.0000E-09	6.5000E-09	7.0000E-09	7.5000E-09	8.0000E-09
8.5000E-09	9.0000E-09	9.5000E-09	1.0000E-08	1.0500E-08	1.1000E-08	1.1500E-08
1.2000E-08	1.2500E-08	1.3000E-08	1.3500E-08	1.4000E-08	1.4500E-08	1.5000E-08
1.5500E-08	1.6000E-08	1.6500E-08	1.7000E-08	1.7500E-08	1.8000E-08	1.8500E-08
1.9000E-08	2.0000E-08	2.1000E-08	2.2000E-08	2.3000E-08	2.4000E-08	2.5000E-08

FOR DETECTOR 4

UPPER LIMITS OF TIME BINS

5.0000E-09	5.5000E-09	6.0000E-09	6.5000E-09	7.0000E-09	7.5000E-09	8.0000E-09
8.5000E-09	9.0000E-09	9.5000E-09	1.0000E-08	1.0500E-08	1.1000E-08	1.1500E-08
1.2000E-08	1.2500E-08	1.3000E-08	1.3500E-08	1.4000E-08	1.4500E-08	1.5000E-08
1.5500E-08	1.6000E-08	1.6500E-08	1.7000E-08	1.7500E-08	1.8000E-08	1.8500E-08
1.9000E-08	2.0000E-08	2.1000E-08	2.2000E-08	2.3000E-08	2.4000E-08	2.5000E-08

NUMBER OF ANGLE BINS 0

UPPER LIMITS OF COSINE BINS

6338 CELLS USED BY ANALYSIS, 939616 CELLS REMAIN UNUSED.

TIME REQUIRED FOR INPUT WAS 1 SECOND(S), 0 MINUTE(S), 0 HOUR(S)

YOU ARE USING THE DEFAULT VERSION OF STRUN WHICH DOES NOTHING.

***START BATCH 1 RANDOM= 0 FA231A

SOURCE DATA

YOU ARE USING THE DEFAULT VERSION OF SOURCE WHICH SETS WAVE TO DDF AND PROVIDES AN ENERGY IG.

WTAVE	WAVE	WAVE	WAVE	XAVE	YAVE	ZAVE	AGEAV
1.000E+03	9.08	0.0356	-0.0159	-0.0083	0.000E+00	0.000E+00	0.000E+00

NUMBER OF COLLISIONS OF TYPE NCOLL

SOURCE SPLIT(0)	FISHN	GAMGEN	REALCOLL	ALBEDO	BDRYX	ESCAPE	E-CUT	TIMEKILL	R R	KILL	R R	SURV	GAMLOST
1000	0	0	0	26114	0	7159	0	0	0	1000	11	0	

TIME REQUIRED FOR THE PRECEDING BATCH WAS 13 SECOND(S), 5 MINUTE(S), 0 HOUR(S)

***START BATCH 2 RANDOM= 0 A7733860

SOURCE DATA

WTAVE	UAVE	UAVE	WAVE	WAVE	XAVE	YAVE	ZAVE	AGEAVE
1.000E+03	9.04	-0.0207	-0.0322	-0.0032	0.000E+00	0.000E+00	0.000E+00	0.000E+00

NUMBER OF COLLISIONS OF TYPE NCOLL

SOURCE SPLIT(0)	FISHN	GAMGEN	REALCOLL	ALBEDO	BDRYX	ESCAPE	E-CUT	TIMEKILL	R R	KILL	R R	SURV	GAMLOST
1000	0	0	0	26707	0	7239	0	0	0	1000	12	0	

TIME REQUIRED FOR THE PRECEDING BATCH WAS 22 SECOND(S), 5 MINUTE(S), 0 HOUR(S)

***START BATCH 3 RANDOM= 0 1D9F1DD3

SOURCE DATA

WTAVE	UAVE	UAVE	WAVE	WAVE	XAVE	YAVE	ZAVE	AGEAVE
1.000E+03	8.96	0.0041	-0.0099	0.0253	0.000E+00	0.000E+00	0.000E+00	0.000E+00

NUMBER OF COLLISIONS OF TYPE NCOLL

SOURCE SPLIT(0)	FISHN	GAMGEN	REALCOLL	ALBEDO	BDRYX	ESCAPE	E-CUT	TIMEKILL	R R	KILL	R R	SURV	GAMLOST
1000	0	0	0	26449	0	7265	0	0	0	1000	6	0	

TIME REQUIRED FOR THE PRECEDING BATCH WAS 18 SECOND(S), 5 MINUTE(S), 0 HOUR(S)

***START BATCH 4 RANDOM= 0 568F0DE97

SOURCE DATA

WTAVE	UAVE	UAVE	WAVE	WAVE	XAVE	YAVE	ZAVE	AGEAVE
1.000E+03	9.03	0.0020	0.0239	0.0278	0.000E+00	0.000E+00	0.000E+00	0.000E+00

NUMBER OF COLLISIONS OF TYPE NCOLL

SOURCE SPLIT(0)	FISHN	GAMGEN	REALCOLL	ALBEDO	BDRYX	ESCAPE	E-CUT	TIMEKILL	R R	KILL	R R	SURV	GAMLOST
1000	0	0	0	26234	0	7270	0	0	0	1000	8	0	

TIME REQUIRED FOR THE PRECEDING BATCH WAS 14 SECOND(S), 5 MINUTE(S), 0 HOUR(S)

***START BATCH 5 RANDOM= 0 42675979

SOURCE DATA

WTAVE	UAVE	UAVE	WAVE	WAVE	XAVE	YAVE	ZAVE	AGEAVE
1.000E+03	8.99	-0.0307	0.0215	0.0191	0.000E+00	0.000E+00	0.000E+00	0.000E+00

NUMBER OF COLLISIONS OF TYPE NCOLL

SOURCE SPLIT(0)	FISHN	GAMGEN	REALCOLL	ALBEDO	BDRYX	ESCAPE	E-CUT	TIMEKILL	R R	KILL	R R	SURV	GAMLOST
1000	0	0	0	25332	0	7133	0	0	0	1000	12	0	

TIME REQUIRED FOR THE PRECEDING BATCH WAS 4 SECOND(S), 5 MINUTE(S), 0 HOUR(S)
TODAY IS 12-13-91

X-Ray Ionization in Silicon {Gy(Si)/source particle (X Ray Dose)}.025cm Kapton

DETECTOR	RESPONSES(DETECTOR) RESULTS of Nova Upgrade calculation -- X-ray Simulation			
	UNCOLL RESPONSE	FSI UNCOLL	TOTAL RESPONSE	FSI TOTAL
1	0.0000E+00	0.00000	1.0797E-16	0.00891
2	0.0000E+00	0.00000	2.9027E-17	0.01201
3	0.0000E+00	0.00000	1.2054E-17	0.01962
4	0.0000E+00	0.00000	1.1732E-17	0.03900

X Ray Fluence (x rays/cm²/source particle)

DETECTOR	RESPONSES(DETECTOR) RESULTS of Nova Upgrade calculation -- X-ray Simulation			
	UNCOLL RESPONSE	FSI UNCOLL	TOTAL RESPONSE	FSI TOTAL
1	0.0000E+00	0.00000	9.5983E-06	0.01463
2	0.0000E+00	0.00000	2.6791E-06	0.01657
3	0.0000E+00	0.00000	1.1406E-06	0.03907
4	0.0000E+00	0.00000	1.1738E-06	0.11790

X Rays (joules/cm²/source photon)

DETECTOR	RESPONSES(DETECTOR) RESULTS of Nova Upgrade calculation -- X-ray Simulation			
	UNCOLL RESPONSE	FSI UNCOLL	TOTAL RESPONSE	FSI TOTAL
1	0.0000E+00	0.00000	4.0044E-20	0.01741
2	0.0000E+00	0.00000	1.1477E-20	0.02189
3	0.0000E+00	0.00000	4.9951E-21	0.06165
4	0.0000E+00	0.00000	5.4309E-21	0.19051

FLUENCE{ENERGY,DETECTOR} {x rays/cm²/eV/source photon}

DETECTOR NO.	1	2	3	4
ENERGIES				
1.000E+06	0.000E+00	0.000E+00	0.000E+00	0.000E+00
	0.000	0.000	0.000	0.000
7.000E+05	0.000E+00	0.000E+00	0.000E+00	0.000E+00
	0.000	0.000	0.000	0.000
4.500E+05	0.000E+00	0.000E+00	0.000E+00	0.000E+00
	0.000	0.000	0.000	0.000
3.000E+05	0.000E+00	0.000E+00	0.000E+00	0.000E+00
	0.000	0.000	0.000	0.000
1.500E+05	3.642E-14	8.932E-15	3.124E-15	2.289E-15
	0.757	0.808	1.000	1.000

1.000E+05	8.099E-13	2.681E-13	9.754E-14	9.783E-14
	0.443	0.339	0.194	0.145
7.000E+04	1.716E-11	5.808E-12	3.261E-12	5.257E-12
	0.120	0.099	0.280	0.585
4.500E+04	1.406E-10	4.164E-11	1.736E-11	1.802E-11
	0.038	0.030	0.048	0.160
3.000E+04	3.841E-10	1.062E-10	4.527E-11	4.410E-11
	0.048	0.026	0.027	0.053
2.000E+04	3.194E-10	8.389E-11	3.431E-11	3.280E-11
	0.015	0.011	0.018	0.035
1.000E+04				

DETECTOR NO 1 RESPONSE(RESPONSE,TIME,DETECTOR) (1-Gy(Si) 2-photons/cm² 3-J/cm² /sec/Source Particle)
 RESPONSE 1 2 3
 TIMES
 5.004E-09 0.000E+00 0.000E+00 0.000E+00
 0.000 0.000 0.000
 5.000E-09 0.000E+00 0.000E+00 0.000E+00
 0.000 0.000 0.000
 5.500E-09 0.000E+00 0.000E+00 0.000E+00
 0.000 0.000 0.000
 6.000E-09 1.810E-08 1.478E+03 6.307E-12
 0.037 0.061 0.000
 6.500E-09 3.964E-08 3.367E+03 1.418E-11
 0.036 0.032 0.000
 7.000E-09 2.472E-08 2.209E+03 9.352E-12
 0.028 0.026 0.000
 7.500E-09 1.270E-08 1.158E+03 4.866E-12
 0.041 0.053 0.000
 8.000E-09 1.149E-08 1.037E+03 4.421E-12
 0.051 0.075 0.000
 8.500E-09 1.345E-08 1.192E+03 4.922E-12
 0.045 0.044 0.000
 9.000E-09 1.433E-08 1.244E+03 4.994E-12
 0.088 0.089 0.000
 9.500E-09 1.144E-08 1.063E+03 4.596E-12
 0.074 0.068 0.000
 1.000E-08 P 167E-09 7.781E+02 3.242E-12
 0.082 0.084 0.000
 1.050E-08 7.004E-09 5.941E+02 2.381E-12
 0.000 0.024 0.000
 1.100E-08 6.326E-09 5.474E+02 2.230E-12
 0.159 0.182 0.000
 1.150E-08 4.861E-09 4.190E+02 1.670E-12
 0.121 0.103 0.000
 1.200E-08 5.079E-09 4.482E+02 1.783E-12
 0.085 0.115 0.000
 1.250E-08

	4.851E-09	4.423E+02	1.813E-12
	0.055	0.060	0.000
1.300E-08			
DETECTOR NO 1	RESPONSE	(RESPONSE,TIME,DETECTOR) (1-Gy(Si) 2-photons/cm ² 3-J/cm ² /sec/Source Particle)	
	1	2	3
TIMES			
1.300E-08	3.433E-09	3.217E+02	1.340E-12
	0.090	0.088	0.000
1.350E-08	4.091E-09	3.970E+02	1.690E-12
	0.136	0.108	0.000
1.400E-08	3.380E-09	3.106E+02	1.275E-12
	0.110	0.108	0.000
1.450E-08	3.206E-09	3.050E+02	1.280E-12
	0.102	0.106	0.000
1.500E-08	2.814E-09	2.694E+02	1.114E-12
	0.095	0.130	0.000
1.550E-08	1.979E-09	1.971E+02	8.107E-13
	0.110	0.138	0.000
1.600E-08	1.864E-09	1.665E+02	6.539E-13
	0.137	0.133	0.000
1.650E-08	1.178E-09	1.110E+02	4.477E-13
	0.000	0.088	0.000
1.700E-08	1.385E-09	1.290E+02	5.501E-13
	0.000	0.083	0.000
1.750E-08	9.951E-10	7.928E+01	2.846E-13
	0.000	0.164	0.000
1.800E-08	1.026E-09	1.136E+02	5.114E-13
	0.000	0.218	0.000
1.850E-08	1.109E-09	1.145E+02	5.185E-13
	0.000	0.190	0.000
1.900E-08	8.218E-10	8.849E+01	3.697E-13
	0.155	0.159	0.000
2.000E-08	6.439E-10	6.767E+01	2.940E-13
	0.000	0.099	0.000
2.100E-08	6.248E-10	5.860E+01	2.268E-13
	0.206	0.201	0.000

2.200E-08 3.711E-10 2.675E+01 9.229E-14
 0.000 0.155 0.000

2.300E-08 1.902E-10 2.048E+01 9.012E-14
 0.000 0.225 0.000

2.400E-08

DETECTOR NO 1 RESPONSE(RESPONSE,TIME,DETECTOR) (1-Gy(S) 2-photons/cm² 3-J/cm² /sec/Source Particle)
 RESPONSE 1 2 3
 TIMES
 2.400E-08 1.895E-11 1.716E+00 6.719E-15
 0.189 0.210 0.000
 7.704E-08

 DETECTOR NO 2 RESPONSE(RESPONSE,TIME,DETECTOR) (1-Gy(S) 2-photons/cm² 3-J/cm² /sec/Source Particle)
 RESPONSE 1 2 3
 TIMES
 8.339E-09 0.000E+00 0.000E+00 0.000E+00
 0.000 0.000 0.000
 5.000E-09 0.000E+00 0.000E+00 0.000E+00
 0.000 0.000 0.000
 5.500E-09 0.000E+00 0.000E+00 0.000E+00
 0.000 0.000 0.000
 6.000E-09 0.000E+00 0.000E+00 0.000E+00
 0.000 0.000 0.000
 6.500E-09 0.000E+00 0.000E+00 0.000E+00
 0.000 0.000 0.000
 7.000E-09 0.000E+00 0.000E+00 0.000E+00
 0.000 0.000 0.000
 7.500E-09 0.000E+00 0.000E+00 0.000E+00
 0.000 0.000 0.000
 8.000E-09 0.000E+00 0.000E+00 0.000E+00
 0.000 0.000 0.000
 8.500E-09 0.000E+00 0.000E+00 0.000E+00
 0.000 0.000 0.000
 9.000E-09 5.831E-09 5.055E+02 2.212E-12
 0.058 0.067 0.000
 9.500E-09 4.448E-09 4.037E+02 1.764E-12
 0.058 0.058 0.000
 1.000E-08 1.048E-08 8.538E+02 3.506E-12
 0.022 0.017 0.000
 1.050E-08 4.969E-09 4.495E+02 1.924E-12
 0.000 0.017 0.000
 1.100E-08 3.933E-09 3.450E+02 1.443E-12

	0.000	0.028	0.000
1.150E-08	3.954E-09	3.529E+02	1.483E-12
	0.000	0.050	0.000
1.200E-08	3.733E-09	3.571E+02	1.545E-12
	0.080	0.088	0.000
1.250E-08	2.964E-09	2.869E+02	1.272E-12
	0.074	0.108	0.000
1.300E-08			

DETECTOR NO 2 RESPONSE(RESPONSE,TIME,DETECTOR) (1-Gy(Si) 2-photons/cm² 3-J/cm² /sec/Source Particle)
 RESPONSE 1 2 3
 TIMES
 1.300E-08 2.053E-09 2.039E+02 8.943E-13
 0.000 0.051 0.000
 1.350E-08 1.760E-09 1.719E+02 7.170E-13
 0.000 0.079 0.000
 1.400E-08 1.437E-09 1.269E+02 5.101E-13
 0.000 0.064 0.000
 1.450E-08 1.583E-09 1.523E+02 6.255E-13
 0.000 0.096 0.000
 1.500E-08 1.376E-09 1.433E+02 6.626E-13
 0.000 0.155 0.000
 1.550E-08 1.134E-09 1.324E+02 6.258E-13
 0.000 0.173 0.000
 1.600E-08 1.143E-09 1.260E+02 5.634E-13
 0.000 0.112 0.000
 1.650E-08 7.512E-10 6.995E+01 2.795E-13
 0.000 0.123 0.000
 1.700E-08 7.096E-10 7.586E+01 3.327E-13
 0.000 0.078 0.000
 1.750E-08 7.451E-10 8.601E+01 4.118E-13
 0.000 0.071 0.000
 1.800E-08 6.025E-10 5.618E+01 2.291E-13
 0.000 0.155 0.000
 1.850E-08 5.704E-10 6.075E+01 2.647E-13
 0.000 0.139 0.000
 1.900E-08 3.937E-10 3.625E+01 1.453E-13
 0.000 0.083 0.000
 2.000E-08 2.937E-10 3.156E+01 1.386E-13
 0.000 0.238 0.000
 2.100E-08 3.203E-10 3.345E+01 1.471E-13
 0.000 0.021 0.000
 2.200E-08 1.857E-10 2.015E+01 8.416E-14
 0.000 0.206 0.000
 2.300E-08

	1.955E-10	2.511E+01	1.182E-13
	0.000	0.311	0.000
2.400E-08			
DETECTOR NO 2	RESPONSE(RESPONSE,TIME,DETECTOR) (1-Gy(Si) 2-photons/cm2 3-J/cm2 /sec/Source Particle)		
RESPONSE	1	2	3
TIMES			
2.400E-08			
	1.029E-11	9.866E-01	3.948E-15
	0.000	0.108	0.000
7.753E-08			
DETECTOR NO 3	RESPONSE(RESPONSE,TIME,DETECTOR) (1-Gy(Si) 2-photons/cm2 3-J/cm2 /sec/Source Particle)		
RESPONSE	1	2	3
TIMES			
1.167E-08			
	0.000E+00	0.000E+00	0.000E+00
	0.000	0.000	0.000
5.000E-09			
	0.000E+00	0.000E+00	0.000E+00
	0.000	0.000	0.000
5.500E-09			
	0.000E+00	0.000E+00	0.000E+00
	0.000	0.000	0.000
6.000E-09			
	0.000E+00	0.000E+00	0.000E+00
	0.000	0.000	0.000
6.500E-09			
	0.000E+00	0.000E+00	0.000E+00
	0.000	0.000	0.000
7.000E-09			
	0.000E+00	0.000E+00	0.000E+00
	0.000	0.000	0.000
7.500E-09			
	0.000E+00	0.000E+00	0.000E+00
	0.000	0.000	0.000
8.000E-09			
	0.000E+00	0.000E+00	0.000E+00
	0.000	0.000	0.000
8.500E-09			
	0.000E+00	0.000E+00	0.000E+00
	0.000	0.000	0.000
9.000E-09			
	0.000E+00	0.000E+00	0.000E+00
	0.000	0.000	0.000
9.500E-09			
	0.000E+00	0.000E+00	0.000E+00
	0.000	0.000	0.000
1.000E-08			
	0.000E+00	0.000E+00	0.000E+00
	0.000	0.000	0.000
1.050E-08			

	0.000E+00	0.000E+00	0.000E+00
	0.000	0.000	0.000
1.100E-08	0.000E+00	0.000E+00	0.000E+00
	0.000	0.000	0.000
1.150E-08	0.000E+00	0.000E+00	0.000E+00
	0.000	0.000	0.000
1.200E-08	1.151E-09	1.056E+02	4.744E-13
	0.000	0.051	0.000
1.250E-08	1.404E-09	1.218E+02	5.362E-13
	0.000	0.080	0.000
1.300E-08			

DETECTOR NO 3 RESPONSE(RESPONSE,TIME,DETECTOR) (1-Gy(Si) 2-photons/cm² 3-J/cm² /sec/Source Particle)

RESPONSE	1	2	3
TIMES			
1.300E-08	3.120E-09	2.661E+02	1.132E-12
	0.000	0.030	0.000
1.350E-08	3.938E-09	3.281E+02	1.354E-12
	0.000	0.022	0.000
1.400E-08	2.082E-09	1.837E+02	7.712E-13
	0.000	0.031	0.000
1.450E-08	2.1E-09	2.010E+02	9.196E-13
	0.000	0.166	0.000
1.500E-08	1.655E-09	1.747E+02	8.375E-13
	0.000	0.138	0.000
1.550E-08	1.397E-09	1.353E+02	5.848E-13
	0.000	0.095	0.000
1.600E-08	9.462E-10	8.892E+01	3.819E-13
	0.000	0.150	0.000
1.650E-08	7.845E-10	9.019E+01	4.450E-13
	0.000	0.194	0.000
1.700E-08	7.613E-10	7.426E+01	3.177E-13
	0.000	0.077	0.000
1.750E-08	6.424E-10	7.045E+01	3.092E-13
	0.000	0.100	0.000
1.800E-08	6.297E-10	6.937E+01	3.109E-13
	0.000	0.204	0.000

1.850E-08	3.842E-10	4.476E+01	2.152E-13
	0.000	0.056	0.000
1.900E-08	3.912E-10	3.943E+01	1.649E-13
	0.000	0.068	0.000
2.000E-08	2.661E-10	2.848E+01	1.309E-13
	0.000	0.214	0.000
2.100E-08	1.877E-10	2.064E+01	9.338E-14
	0.000	0.151	0.000
2.200E-08	1.714E-10	1.658E+01	6.870E-14
	0.000	0.217	0.000
2.300E-08	9.155E-11	8.575E+00	3.541E-14
	0.000	0.129	0.000
2.400E-08			

DETECTOR NO 3 RESPONSE(RESPONSE,TIME,DETECTOR) (1-Gy(Si) 2-photons/cm² 3-J/cm² /sec/Source Particle)

RESPONSE	1	2	3
----------	---	---	---

TIMES

2.400E-08	8.896E-12	9.100E-01	3.781E-15
	0.000	0.102	0.000
7.881E-08			

DETECTOR NO 4 RESPONSE(RESPONSE,TIME,DETECTOR) (1-Gy(Si) 2-photons/cm² 3-J/cm² /sec/Source Particle)

RESPONSE	1	2	3
----------	---	---	---

TIMES

1.182E-08	0.000E+00	0.000E+00	0.000E+00
	0.000	0.000	0.000
5.000E-09	0.000E+00	0.000E+00	0.000E+00
	0.000	0.000	0.000
5.500E-09	0.000E+00	0.000E+00	0.000E+00
	0.000	0.000	0.000
6.000E-09	0.000E+00	0.000E+00	0.000E+00
	0.000	0.000	0.000
6.500E-09	0.000E+00	0.000E+00	0.000E+00
	0.000	0.000	0.000
7.000E-09	0.000E+00	0.000E+00	0.000E+00
	0.000	0.000	0.000
7.500E-09	0.000E+00	0.000E+00	0.000E+00
	0.000	0.000	0.000

8.000E-09	0.000E+00	0.000E+00	0.000E+00
	0.000	0.000	0.000
8.500E-09	0.000E+00	0.000E+00	0.000E+00
	0.000	0.000	0.000
9.000E-09	0.000E+00	0.000E+00	0.000E+00
	0.000	0.000	0.000
9.500E-09	0.000E+00	0.000E+00	0.000E+00
	0.000	0.000	0.000
1.000E-08	0.000E+00	0.000E+00	0.000E+00
	0.000	0.000	0.000
1.050E-08	0.000E+00	0.000E+00	0.000E+00
	0.000	0.000	0.000
1.100E-08	0.000E+00	0.000E+00	0.000E+00
	0.000	0.000	0.000
1.150E-08	1.281E-11	5.667E-01	1.362E-15
	0.000	1.000	0.000
1.200E-08	2.921E-10	2.841E+01	1.264E-13
	0.000	0.152	0.000
1.250E-08	1.271E-09	2.154E+02	1.458E-12
	0.197	0.576	0.000
1.300E-08			

DETECTOR NO	4	RESPONSE	(RESPONSE,TIME,DETECTOR) (1-Gy(Si) 2-photons/cm ² 3-J/cm ² /sec/Source Particle)	
RESPONSE		1	2	3
TIMES				
1.300E-08		2.319E-09	2.260E+02	1.094E-12
		0.000	0.178	0.000
1.350E-08		4.592E-09	3.833E+02	1.609E-12
		0.000	0.019	0.000
1.400E-08		2.772E-09	2.422E+02	1.025E-12
		0.165	0.139	0.000
1.450E-08		1.782E-09	1.923E+02	9.180E-13
		0.000	0.263	0.000
1.500E-08		1.535E-09	1.359E+02	5.689E-13
		0.000	0.057	0.000
1.550E-08		1.434E-09	1.503E+02	6.737E-13

	0.000	0.100	0.000
1.600E-08	9.495E-10	7.60E+01	3.665E-13
	0.000	0.094	0.000
1.650E-08	8.118E-10	8.697E+01	4.039E-13
	0.000	0.245	0.000
1.700E-08	6.172E-10	6.514E+01	3.126E-13
	0.000	0.150	0.000
1.750E-08	8.788E-10	8.863E+01	3.516E-13
	0.318	0.358	0.000
1.800E-08	5.348E-10	5.619E+01	2.450E-13
	0.000	0.107	0.000
1.850E-08	3.901E-10	3.906E+01	1.757E-13
	0.000	0.122	0.000
1.900E-08	4.372E-10	4.944E+01	2.206E-13
	0.000	0.234	0.000
2.000E-08	2.488E-10	2.863E+01	1.429E-13
	0.000	0.175	0.000
2.100E-08	1.766E-10	1.865E+01	8.090E-14
	0.000	0.082	0.000
2.200E-08	1.489E-10	1.463E+01	6.329E-14
	0.000	0.105	0.000
2.300E-08	1.845E-10	1.949E+01	7.791E-14
	0.000	0.544	0.000
2.400E-08			

DETECTOR NO 4 RESPONSE(RESPONSE,TIME,DETECTOR) (1-Gy(Si) 2-photons/cm² 3-J/cm² /sec/Source Particle)

RESPONSE	1	2	3
----------	---	---	---

TIMES

2.400E-08

7.994E-12	7.984E-01	3.275E-15
0.000	0.075	0.000

7.906E-08

DETECTOR NO 1 FLUENCE(TIME,ENERGY,DETECTOR) (photons/cm²/eV/sec/source photon)

ENERGIES	1.000E+06	7.000E+05	4.500E+05	3.000E+05	1.500E+05	1.000E+05	7.000E+04	4.500E+04	3.000E+04	2.000E+04
TIMES	7.000E+05	4.500E+05	3.000E+05	1.500E+05	1.000E+05	7.000E+04	4.500E+04	3.000E+04	2.000E+04	1.000E+04
5.004E-09	0.000E+00									
	0.000	0.000	0.000	0.000	0.000	0.000	0.000	0.000	0.000	0.000
5.000E-09										

	0.000E+00									
5.500E-09	0.000	0.000	0.000	0.000	0.000	0.000	0.000	0.000	0.000	0.000
	0.000E+00									
6.000E-09	0.000	0.000	0.000	0.000	0.000	0.000	0.000	0.000	0.000	0.000
	0.000E+00	0.000E+00	0.000E+00	0.000E+00	3.182E-05	3.962E-04	4.982E-03	1.889E-02	4.525E-02	6.041E-02
6.500E-09	0.000	0.000	0.000	0.000	1.000	0.459	0.181	0.111	0.099	0.028
	0.000E+00	0.000E+00	0.000E+00	0.000E+00	1.590E-05	6.694E-04	7.100E-03	5.312E-02	1.104E-01	1.268E-01
7.000E-09	0.000	0.000	0.000	0.000	1.000	0.695	0.084	0.071	0.097	0.036
	0.000E+00	0.000E+00	0.000E+00	0.000E+00	2.511E-05	1.446E-04	5.144E-03	3.162E-02	8.656E-02	7.352E-02
7.500E-09	0.000	0.000	0.000	0.000	1.000	0.485	0.255	0.052	0.035	0.036
	0.000E+00	0.000E+00	0.000E+00	0.000E+00	7.964E-06	2.662E-03	1.530E-02	4.998E-02	3.617E-02	
8.000E-09	0.000	0.000	0.000	0.000	0.000	0.613	0.110	0.117	0.069	0.049
	0.000E+00	0.000E+00	0.000E+00	0.000E+00	6.601E-05	2.769E-03	1.444E-02	4.096E-02	3.392E-02	
8.500E-09	0.000	0.000	0.000	0.000	0.000	0.596	0.369	0.174	0.083	0.041
	0.000E+00	0.000E+00	0.000E+00	0.000E+00	3.331E-06	2.165E-03	1.647E-02	4.970E-02	3.941E-02	
9.000E-09	0.000	0.000	0.000	0.000	0.000	0.838	0.183	0.133	0.131	0.044
	0.000E+00	0.000E+00	0.000E+00	0.000E+00	0.000E+00	1.025E-03	1.867E-02	5.127E-02	4.251E-02	
9.500E-09	0.000	0.000	0.000	0.000	0.000	0.216	0.081	0.129	0.088	
	0.000E+00	0.000E+00	0.000E+00	0.000E+00	0.000E+00	2.652E-04	1.856E-03	1.853E-02	3.965E-02	3.339E-02
1.000E-08	0.000	0.000	0.000	0.000	0.000	0.871	0.439	0.080	0.094	0.087
	0.000E+00	0.000E+00	0.000E+00	0.000E+00	0.000E+00	6.020E-04	1.329E-02	3.441E-02	2.196E-02	
1.050E-08	0.000	0.000	0.000	0.000	0.000	0.306	0.206	0.097	0.110	
	0.000E+00	0.000E+00	0.000E+00	0.000E+00	0.000E+00	6.712E-05	5.489E-04	8.383E-03	2.400E-02	2.126E-02
1.100E-08	0.000	0.000	0.000	0.000	0.000	0.922	0.402	0.186	0.060	0.049
	0.000E+00	0.000E+00	0.000E+00	0.000E+00	0.000E+00	8.882E-04	7.520E-03	2.228E-02	1.897E-02	
1.150E-08	0.000	0.000	0.000	0.000	0.000	0.581	0.226	0.201	0.151	
	0.000E+00	0.000E+00	0.000E+00	0.000E+00	0.000E+00	4.263E-04	5.514E-03	1.828E-02	1.429E-02	
1.200E-08	0.000	0.000	0.000	0.000	0.000	0.620	0.243	0.143	0.141	
	0.000E+00	0.000E+00	0.000E+00	0.000E+00	0.000E+00	4.138E-04	5.428E-03	2.138E-02	1.426E-02	
1.250E-08	0.000	0.000	0.000	0.000	0.000	0.383	0.303	0.171	0.154	
	0.000E+00	0.000E+00	0.000E+00	0.000E+00	0.000E+00	6.004E-04	5.952E-03	2.035E-02	1.345E-02	
1.300E-08	0.000	0.000	0.000	0.000	0.000	0.221	0.215	0.240	0.112	

DETECTOR NO 1 FLUENCE(TIME,ENERGY,DETECTOR) (photons/cm²/eV/sec/source photon)

ENERGIES 1.000E+06 7.000E+05 4.500E+05 3.000E+05 1.500E+05 1.000E+05 7.000E+04 4.500E+04 3.000E+04 2.000E+04

TIMES	7.000E+05	4.500E+05	3.000E+05	1.500E+05	1.000E+05	7.000E+04	4.500E+04	3.000E+04	2.000E+04	1.000E+04
1.300E-08	0.000E+00	0.000E+00	0.000E+00	0.000E+00	0.000E+00	0.000E+00	1.289E-04	6.312E-03	1.272E-02	9.666E-03
	0.000	0.000	0.000	0.000	0.000	0.000	0.922	0.181	0.093	0.113
1.350E-08	0.000E+00	0.000E+00	0.000E+00	0.000E+00	0.000E+00	0.000E+00	4.577E-04	7.219E-03	1.669E-02	1.104E-02
	0.000	0.000	0.000	0.000	0.000	0.000	0.630	0.214	0.147	0.172
1.400E-08	0.000E+00	0.000E+00	0.000E+00	0.000E+00	0.000E+00	0.000E+00	2.558E-04	4.940E-03	1.359E-02	9.417E-03
	0.000	0.000	0.000	0.000	0.000	0.000	0.524	0.225	0.225	0.093
1.450E-08	0.000E+00	0.000E+00	0.000E+00	0.000E+00	0.000E+00	0.000E+00	5.434E-04	4.134E-03	1.445E-02	8.496E-03
	0.000	0.000	0.000	0.000	0.000	0.000	0.454	0.162	0.219	0.114
1.500E-08	0.000E+00	0.000E+00	0.000E+00	0.000E+00	0.000E+00	0.000E+00	2.621E-04	3.904E-03	1.315E-02	7.279E-03
	0.000	0.000	0.000	0.000	0.000	0.000	0.806	0.303	0.158	0.141
1.550E-08	0.000E+00	0.000E+00	0.000E+00	0.000E+00	0.000E+00	0.000E+00	1.925E-05	3.165E-03	1.016E-02	4.760E-03
	0.000	0.000	0.000	0.000	0.000	0.000	1.000	0.422	0.233	0.135
1.600E-08	0.000E+00	0.000E+00	0.000E+00	0.000E+00	0.000E+00	0.000E+00	2.472E-05	2.173E-03	8.244E-03	5.087E-03
	0.000	0.000	0.000	0.000	0.000	0.000	1.000	0.506	0.210	0.179
1.650E-08	0.000E+00	0.000E+00	0.000E+00	0.000E+00	0.000E+00	0.000E+00	9.337E-05	1.281E-03	5.976E-03	2.970E-03
	0.000	0.000	0.000	0.000	0.000	0.000	0.650	0.383	0.346	0.218
1.700E-08	0.000E+00	0.000E+00	0.000E+00	0.000E+00	0.000E+00	0.000E+00	2.899E-04	1.959E-03	5.302E-03	3.931E-03
	0.000	0.000	0.000	0.000	0.000	0.000	0.672	0.268	0.242	0.258
1.750E-08	0.000E+00	0.000E+00	0.000E+00	0.000E+00	0.000E+00	0.000E+00	3.241E-05	2.780E-04	4.592E-03	2.838E-03
	0.000	0.000	0.000	0.000	0.000	0.000	0.711	0.232	0.290	0.215
1.800E-08	0.000E+00	0.000E+00	0.000E+00	0.000E+00	0.000E+00	0.000E+00	1.708E-04	2.405E-03	4.943E-03	2.384E-03
	0.000	0.000	0.000	0.000	0.000	0.000	0.566	0.625	0.245	0.091
1.850E-08	0.000E+00	0.000E+00	0.000E+00	0.000E+00	0.000E+00	0.000E+00	5.471E-04	1.066E-03	5.782E-03	2.701E-03
	0.000	0.000	0.000	0.000	0.000	0.000	0.897	0.481	0.224	0.109
1.900E-08	0.000E+00	0.000E+00	0.000E+00	0.000E+00	0.000E+00	0.000E+00	2.989E-05	1.264E-03	5.224E-03	1.655E-03
	0.000	0.000	0.000	0.000	0.000	0.000	0.738	0.282	0.244	0.245
2.000E-08	0.000E+00	0.000E+00	0.000E+00	0.000E+00	0.000E+00	0.000E+00	7.160E-05	1.276E-03	3.132E-03	1.542E-03
	0.000	0.000	0.000	0.000	0.000	0.000	0.815	0.299	0.169	0.113
2.100E-08	0.000E+00	0.000E+00	0.000E+00	0.000E+00	0.000E+00	0.000E+00	3.058E-06	5.130E-04	3.607E-03	1.476E-03
	0.000	0.000	0.000	0.000	0.000	0.000	1.000	0.483	0.304	0.193
2.200E-08	0.000E+00	0.000E+00	0.000E+00	0.000E+00	0.000E+00	0.000E+00	1.959E-05	5.110E-05	1.368E-03	1.181E-03
	0.000	0.000	0.000	0.000	0.000	0.000	0.780	0.469	0.244	0.253
2.300E-08	0.000E+00	0.000E+00	0.000E+00	0.000E+00	0.000E+00	0.000E+00	1.214E-05	4.605E-04	8.704E-04	4.568E-04
	0.000	0.000	0.000	0.000	0.000	0.000	0.834	0.632	0.119	0.416

2.400E-08

DETECTOR NO 1 FLUENCE(TIME,ENERGY,DETECTOR) (photons/cm²/eV/sec/source photon)

ENERGIES	1.000E+06	7.000E+05	4.500E+05	3.000E+05	1.500E+05	1.000E+05	7.000E+04	4.500E+04	3.000E+04	2.000E+04
TIMES	7.000E+05	4.500E+05	3.000E+05	1.500E+05	1.000E+05	7.000E+04	4.500E+04	3.000E+04	2.000E+04	1.000E+04
2.400E-08	0.000E+00	0.000E+00	0.000E+00	0.000E+00	0.000E+00	0.000E+00	4.385E-07	1.955E-05	9.142E-05	4.974E-05
7.704E-08	0.000	0.000	0.000	0.000	0.000	0.000	0.383	0.660	0.391	0.184

DETECTOR NO 2 FLUENCE(TIME,ENERGY,DETECTOR) (photons/cm²/eV/sec/source photon)

ENERGIES	1.000E+06	7.000E+05	4.500E+05	3.000E+05	1.500E+05	1.000E+05	7.000E+04	4.500E+04	3.000E+04	2.000E+04
TIMES	7.000E+05	4.500E+05	3.000E+05	1.500E+05	1.000E+05	7.000E+04	4.500E+04	3.000E+04	2.000E+04	1.000E+04
8.339E-09	0.000E+00									
	0.000	0.000	0.000	0.000	0.000	0.000	0.000	0.000	0.000	0.000
5.000E-09	0.000E+00									
	0.000	0.000	0.000	0.000	0.000	0.000	0.000	0.000	0.000	0.000
5.500E-09	0.000E+00									
	0.000	0.000	0.000	0.000	0.000	0.000	0.000	0.000	0.000	0.000
6.000E-09	0.000E+00									
	0.000	0.000	0.000	0.000	0.000	0.000	0.000	0.000	0.000	0.000
6.500E-09	0.000E+00									
	0.000	0.000	0.000	0.000	0.000	0.000	0.000	0.000	0.000	0.000
7.000E-09	0.000E+00									
	0.000	0.000	0.000	0.000	0.000	0.000	0.000	0.000	0.000	0.000
7.500E-09	0.000E+00									
	0.000	0.000	0.000	0.000	0.000	0.000	0.000	0.000	0.000	0.000
8.000E-09	0.000E+00									
	0.000	0.000	0.000	0.000	0.000	0.000	0.000	0.000	0.000	0.000
8.500E-09	0.000E+00									
	0.000	0.000	0.000	0.000	0.000	0.000	0.000	0.000	0.000	0.000
9.000E-09	0.000E+00	0.000E+00	0.000E+00	0.000E+00	1.489E-05	2.502E-04	1.364E-03	7.431E-03	1.664E-02	1.853E-02
	0.000	0.000	0.000	0.000	1.000	0.329	0.156	0.081	0.184	0.060
9.500E-09	0.000E+00	0.000E+00	0.000E+00	0.000E+00	6.836E-05	1.224E-03	6.118E-03	1.449E-02	1.344E-02	
	0.000	0.000	0.000	0.000	0.000	0.701	0.221	0.069	0.098	0.060
1.000E-08	0.000E+00	0.000E+00	0.000E+00	0.000E+00	2.970E-06	5.650E-05	2.102E-03	1.142E-02	2.853E-02	3.427E-02
	0.000	0.000	0.000	0.000	1.000	0.484	0.101	0.033	0.047	0.027
1.050E-08	0.000E+00	0.000E+00	0.000E+00	0.000E+00	3.299E-05	1.125E-03	6.798E-03	1.706E-02	1.478E-02	
	0.000	0.000	0.000	0.000	0.000	0.703	0.149	0.116	0.090	0.021
1.100E-08	0.000E+00	0.000E+00	0.000E+00	0.000E+00	7.931E-06	7.989E-04	4.840E-03	1.334E-02	1.188E-02	
	0.000	0.000	0.000	0.000	0.000	0.649	0.362	0.081	0.068	0.028
1.150E-08	0.000E+00	0.000E+00	0.000E+00	0.000E+00	1.106E-05	7.020E-04	5.453E-03	1.353E-02	1.180E-02	
	0.000	0.000	0.000	0.000	0.000	0.954	0.231	0.169	0.101	0.026
1.200E-08	0.000E+00	0.000E+00	0.000E+00	0.000E+00	8.411E-05	4.895E-04	6.483E-03	1.406E-02	1.045E-02	
	0.000	0.000	0.000	0.000	0.000	0.970	0.274	0.128	0.080	0.084

1.250E-08	0.000E+00 0.000E+00 0.000E+00 0.000E+00 0.000E+00 5.723E-06 8.766E-04 4.680E-03 1.112E-02 8.343E-03
	0.000 0.000 0.000 0.000 0.000 1.000 0.492 0.193 0.118 0.099
1.300E-08	
DETECTOR NO 2	FLUENCE(TIME,ENERGY,DETECTOR) (photons/cm ² /eV/sec/source photon)
ENERGIES	1.000E+06 7.000E+05 4.500E+05 3.000E+05 1.500E+05 1.000E+05 7.000E+04 4.500E+04 3.000E+04 2.000E+04
TIMES	7.000E+05 4.500E+05 3.000E+05 1.500E+05 1.000E+05 7.000E+04 4.500E+04 3.000E+04 2.000E+04 1.000E+04
1.300E-08	0.000E+00 0.000E+00 0.000E+00 0.000E+00 0.000E+00 1.860E-05 5.718E-04 2.770E-03 9.428E-03 5.319E-03
	0.000 0.000 0.000 0.000 0.000 0.995 0.611 0.189 0.099 0.065
1.350E-08	0.000E+00 0.000E+00 0.000E+00 0.000E+00 0.000E+00 6.518E-07 1.404E-04 2.717E-03 8.290E-03 4.475E-03
	0.000 0.000 0.000 0.000 0.000 1.000 0.408 0.222 0.125 0.075
1.400E-08	0.000E+00 0.000E+00 0.000E+00 0.000E+00 0.000E+00 1.434E-04 1.627E-03 5.793E-03 4.095E-03
	0.000 0.000 0.000 0.000 0.000 0.000 0.456 0.208 0.096 0.067
1.450E-08	0.000E+00 0.000E+00 0.000E+00 0.000E+00 0.000E+00 1.522E-04 1.979E-03 7.905E-03 3.974E-03
	0.000 0.000 0.000 0.000 0.000 0.000 0.360 0.248 0.171 0.160
1.500E-08	0.000E+00 0.000E+00 0.000E+00 0.000E+00 0.000E+00 5.027E-04 2.753E-03 5.235E-03 3.709E-03
	0.000 0.000 0.000 0.000 0.000 0.000 0.860 0.282 0.257 0.123
1.550E-08	0.000E+00 0.000E+00 0.000E+00 0.000E+00 0.000E+00 3.877E-04 2.875E-03 5.375E-03 2.584E-03
	0.000 0.000 0.000 0.000 0.000 0.000 0.589 0.207 0.208 0.111
1.600E-08	0.000E+00 0.000E+00 0.000E+00 0.000E+00 0.000E+00 1.233E-04 2.858E-03 5.310E-03 2.693E-03
	0.000 0.000 0.000 0.000 0.000 0.000 0.674 0.219 0.207 0.130
1.650E-08	0.000E+00 0.000E+00 0.000E+00 0.000E+00 0.000E+00 6.643E-07 1.022E-03 3.496E-03 1.963E-03
	0.000 0.000 0.000 0.000 0.000 0.000 0.984 0.309 0.160 0.144
1.700E-08	0.000E+00 0.000E+00 0.000E+00 0.000E+00 0.000E+00 6.157E-05 1.600E-03 3.334E-03 1.699E-03
	0.000 0.000 0.000 0.000 0.000 0.000 0.555 0.277 0.070 0.079
1.750E-08	0.000E+00 0.000E+00 0.000E+00 0.000E+00 0.000E+00 2.758E-04 2.019E-03 3.063E-03 1.821E-03
	0.000 0.000 0.000 0.000 0.000 0.000 0.301 0.241 0.142 0.139
1.800E-08	0.000E+00 0.000E+00 0.000E+00 0.000E+00 0.000E+00 5.731E-05 7.358E-04 2.780E-03 1.591E-03
	0.000 0.000 0.000 0.000 0.000 0.000 0.737 0.348 0.257 0.128
1.850E-08	0.000E+00 0.000E+00 0.000E+00 0.000E+00 0.000E+00 8.898E-05 1.026E-03 3.004E-03 1.309E-03
	0.000 0.000 0.000 0.000 0.000 0.000 1.000 0.535 0.161 0.233
1.900E-08	0.000E+00 0.000E+00 0.000E+00 0.000E+00 0.000E+00 1.299E-05 5.070E-04 1.783E-03 1.049E-03
	0.000 0.000 0.000 0.000 0.000 0.000 0.646 0.364 0.106 0.188
2.000E-08	0.000E+00 0.000E+00 0.000E+00 0.000E+00 0.000E+00 6.603E-05 4.679E-04 1.634E-03 6.550E-04
	0.000 0.000 0.000 0.000 0.000 0.000 0.497 0.466 0.192 0.201
2.100E-08	

	0.000E+00	0.000E+00	0.000E+00	0.000E+00	0.000E+00	0.000E+00	8.336E-05	4.835E-04	1.650E-03	7.617E-04
	0.000	0.000	0.000	0.000	0.000	0.000	0.683	0.204	0.087	0.161
2.200E-08										
	0.000E+00	0.000E+00	0.000E+00	0.000E+00	0.000E+00	0.000E+00	4.413E-06	2.914E-04	1.200E-03	3.664E-04
	0.000	0.000	0.000	0.000	0.000	0.000	0.647	0.443	0.329	0.122
2.300E-08										
	0.000E+00	0.000E+00	0.000E+00	0.000E+00	0.000E+00	0.000E+00	3.795E-05	6.123E-04	1.143E-03	3.548E-04
	0.000	0.000	0.000	0.000	0.000	0.000	0.661	0.756	0.201	0.159
2.400E-08										

DETECTOR NO 2 FLUENCE(TIME,ENERGY,DETECTOR) (photons/cm²/eV/sec/source photon)

ENERGIES	1.000E+06	7.000E+05	4.500E+05	3.000E+05	1.500E+05	1.000E+05	7.000E+04	4.500E+04	3.000E+04	2.000E+04
TIMES	7.000E+05	4.500E+05	3.000E+05	1.500E+05	1.000E+05	7.000E+04	4.500E+04	3.000E+04	2.000E+04	1.000E+04
2.400E-08										
	0.000E+00	0.000E+00	0.000E+00	0.000E+00	0.000E+00	1.117E-10	1.755E-07	1.248E-05	5.448E-05	2.502E-05
	0.000	0.000	0.000	0.000	0.000	0.977	0.614	0.511	0.200	0.087
7.753E-08										
ENERGIES	1.000E+06	7.000E+05	4.500E+05	3.000E+05	1.500E+05	1.000E+05	7.000E+04	4.500E+04	3.000E+04	2.000E+04
TIMES	7.000E+05	4.500E+05	3.000E+05	1.500E+05	1.000E+05	7.000E+04	4.500E+04	3.000E+04	2.000E+04	1.000E+04
2.400E-08										
	0.000E+00	0.000E+00	0.000E+00	0.000E+00	0.000E+00	2.740E-10	5.153E-07	1.307E-05	4.993E-05	2.017E-05
	0.000	0.000	0.000	0.000	0.000	0.999	0.919	0.519	0.087	0.105
7.881E-08										

EXTRA ARRAYS OF LENGTH ND

.....(4)
(-1)

TIME REQUIRED FOR THE PRECEDING 5 BATCHES WAS 15 SECOND(S), 26 MINUTE(S), 0 HOUR(S)

NEUTRON DEATHS	NUMBER	WEIGHT
KILLED BY RUSSIAN ROULETTE	5000	4.74511E+01
ESCAPED	0	0.00000E+00
REACHED ENERGY CUTOFF	0	0.00000E+00
REACHED TIME CUTOFF	0	0.00000E+00

NUMBER OF SCATTERINGS

MEDIUM	NUMBER
1	0
2	8
3	40
4	19128
5	3391

6	241
7	0
8	108028
TOTAL	130836

REAL SCATTERING COUNTERS

ENERGY GROUP	REGION 1	REGION 2	REGION 3	
	NUMBER	WEIGHT	NUMBER	WEIGHT
1	0	0.00E+00	0	0.00E+00
2	0	0.00E+00	0	0.00E+00
3	0	0.00E+00	0	0.00E+00
4	0	0.00E+00	0	0.00E+00
5	0	0.00E+00	4	4.00E+00
6	6	5.21E+00	103	1.03E+02
7	234	1.35E+02	1885	1.83E+03
8	582	3.29E+02	9099	8.11E+03
9	703	3.90E+02	22311	1.49E+04
10	1536	2.21E+02	94373	1.45E+04

NUMBER OF SPLITTINGS

ENERGY GROUP	REGION 1	REGION 2	REGION 3	
	NUMBER	WEIGHT	NUMBER	WEIGHT
1	0	0.00E+00	0	0.00E+00
2	0	0.00E+00	0	0.00E+00
3	0	0.00E+00	0	0.00E+00
4	0	0.00E+00	0	0.00E+00
5	0	0.00E+00	0	0.00E+00
6	0	0.00E+00	0	0.00E+00
7	0	0.00E+00	0	0.00E+00
8	0	0.00E+00	0	0.00E+00
9	0	0.00E+00	0	0.00E+00
10	0	0.00E+00	0	0.00E+00

NUMBER OF SPLITTINGS PREVENTED BY LACK OF ROOM

ENERGY GROUP	REGION 1	REGION 2	REGION 3	
	NUMBER	WEIGHT	NUMBER	WEIGHT
1	0	0.00E+00	0	0.00E+00
2	0	0.00E+00	0	0.00E+00
3	0	0.00E+00	0	0.00E+00
4	0	0.00E+00	0	0.00E+00
5	0	0.00E+00	0	0.00E+00
6	0	0.00E+00	0	0.00E+00
7	0	0.00E+00	0	0.00E+00
8	0	0.00E+00	0	0.00E+00
9	0	0.00E+00	0	0.00E+00
10	0	0.00E+00	0	0.00E+00

NUMBER OF RUSSIAN ROULETTE KILLS

ENERGY	REGION 1		REGION 2		REGION 3	
GROUP	NUMBER	WEIGHT	NUMBER	WEIGHT	NUMBER	WEIGHT
1	0	0.00E+00	0	0.00E+00	0	0.00E+00
2	0	0.00E+00	0	0.00E+00	0	0.00E+00
3	0	0.00E+00	0	0.00E+00	0	0.00E+00
4	0	0.00E+00	0	0.00E+00	0	0.00E+00
5	0	0.00E+00	0	0.00E+00	0	0.00E+00
6	1	2.63E-02	0	0.00E+00	0	0.00E+00
7	37	2.45E+00	0	0.00E+00	0	0.00E+00
8	257	1.22E+01	9	5.57E-05	0	0.00E+00
9	620	2.66E+01	75	2.90E-04	0	0.00E+00
10	1559	6.20E+00	2442	1.53E-02	0	0.00E+00

NUMBER OF RUSSIAN ROULETTE SURVIVALS

ENERGY	REGION 1		REGION 2		REGION 3	
GROUP	NUMBER	WEIGHT	NUMBER	WEIGHT	NUMBER	WEIGHT
1	0	0.00E+00	0	0.00E+00	0	0.00E+00
2	0	0.00E+00	0	0.00E+00	0	0.00E+00
3	0	0.00E+00	0	0.00E+00	0	0.00E+00
4	0	0.00E+00	0	0.00E+00	0	0.00E+00
5	0	0.00E+00	0	0.00E+00	0	0.00E+00
6	0	0.00E+00	0	0.00E+00	0	0.00E+00
7	5	4.04E-01	0	0.00E+00	0	0.00E+00
8	12	6.76E-01	0	0.00E+00	0	0.00E+00
9	22	1.40E+00	0	0.00E+00	0	0.00E+00
10	10	5.55E-01	0	0.00E+00	0	0.00E+00

** NEXT RANDOM NUMBER IS 0 911E02C

TOTAL CPU TIME FOR THIS PROBLEM WAS 26.26 MINUTES.

***** Nova Upgrade X-Ray Effects Simulation 91 *****
 TODAY IS 12-13-91
 END OF FILE READ BY INPUT1, LINE 42
 NORMAL COMPLETION OF JOB

Appendix D: Example of XCHECKER Data Input File

0 8 46 69
46 N. 23 GAMMA (P3) for Nova Upgrade Weapons Effects
46 46 23 23 69 72 4 8 21 37 4 2 1
0 0 0 0 0 0 10 29 0 0
1 2 3 4 43 44 45 46 49 50 51 52 55 56
57 58 37 38 39 40 67 68 69 70 91 92 93 94
97 98 99 100 301 302 303 304 307 308 309 310 313 314
315 316 319 320 321 322 25 26 27 28 31 32 33 34
79 80 81 82 85 86 87 88 133 134 135 136 349 350
351 352 61 62 63 64 157 158 159 160 151 152 153 154
1 13 1.3690-3 Li6 \
1 14 1.6880-2 Li7 \
1 2 3.6320-3 B10 > Lithium Boro-Hydrate 95.6%
1 3 1.4620-2 B11 / enriched
1 -1 7.3000-2 H 1 /
2 1 4.2660-2 H 1 \ 1 H 1
2 2 4.679 -4 B10 43 \ 2 B10 43
2 3 1.965 -3 B11 49 \ 3 B11 49
2 4 2.165 -2 C 55 \ 4 C 55
2 6 5.6930-3 O 67 \ 5 Be9 37
2 7 4.687 -5 Al > Pb-B-Poly 6 0 67
2 8 3.6920-4 Si 97 / 7 Al 91
2 15 3.741 -4 Na 79 / 8 Si 97
2 16 1.977 -4 Mg 85 / 9 W182 301
2 17 6.689 -4 Co 133 / 10 W183 307
2 -18 9.9280-3 Pb 349 / 11 W184 313
3 19 4.3807-3 N 61 \ 12 W186 319
3 4 4.8169-2 C 55 > Kapton 13 Li6 25
3 1 3.9426-2 H 1 / 14 Li7 31
3 -6 1.0952-2 O 67 / 15 Na 79
4 1 7.94 -2 H 1 \ 16 Mg 85
4 2 6.30 -4 B10 43 \ 17 Co 133
4 3 2.52 -3 B11 49 > 5%-B Poly 18 Pb 349
4 -4 3.97 -2 C 55 / 19 N 61
5 7 5.643 -2 Al 91 \ 20 Mn 157
5 20 4.1712-4 Mn 157 \ 21 Cr 151
5 16 2.622 -3 Mg 85 > Al 5083
5 -21 8.930 -5 Cr 151 /
6 9 1.67 -2 W182 301 \
6 10 9.06 -3 W183 307 \
6 11 1.94 -2 W184 313 > Tungsten
6 -12 1.81e -2 W186 319 /
7 1 7.94 -2 H 1 > Polyethylene
7 -4 3.97 -2 C 55 /
8 1 5.845 -2 H \
8 13 5.588 -2 Li6 25 > LiH 95.6% enriched
8 -14 2.572 -3 Li7 31 /
0 8 10 10

Lower 10 X Ray groups (P3) for Nova Upgrade Weapons Effects

0	0	10	10	69	72	4	8	21	37	4	2	1	3
0	0	0	0	0	0	0	10	30	0	0			
1	2	3	4	43	44	45	46	49	50	51	52	55	56
57	58	37	38	39	40	67	68	69	70	91	92	93	94
97	98	99	100	301	302	303	304	307	308	309	310	313	314
315	316	319	320	321	322	25	26	27	28	31	32	33	34
79	80	81	82	85	86	87	88	133	134	135	136	349	350
351	352	61	62	63	64	157	158	159	160	151	152	153	154
1	13	1.3690-3			Li6	\							
1	14	1.6880-2			Li7	\							
1	2	3.6320-3			B10	> Lithium Boro-Hydrate 95.6%							
1	3	1.4620-2			B11	/ enriched							
1	-1	7.3000-2			H 1	/							
2	1	4.2660-2			H 1	\		1	H	1			
2	2	4.679 -4			B10 43	\		2	B10	43			
2	3	1.965 -3			B11 49	\		3	B11	49			
2	4	2.165 -2			C 55	\		4	C	55			
2	6	5.6930-3			O 67	\		5	Be9	37			
2	7	4.687 -5			Al	> Pb-B-Poly	6	0	67				
2	8	3.6920-4			Si 97	/		7	N	91			
2	15	3.741 -4			No 79	/		8	Si	97			
2	16	1.977 -4			Mg 85	/		9	W182	301			
2	17	6.689 -4			Co 133	/		10	W183	307			
2	-18	9.9280-3			Pb 349	/		11	W184	313			
3	19	4.3807-3			N 61	\		12	W186	319			
3	4	4.8169-2			C 55	> Kapton		13	Li6	25			
3	1	3.9426-2			H 1	/		14	Li7	31			
3	-6	1.0952-2			O 67	/		15	No	79			
4	1	7.94 -2			H 1	\		16	Mg	85			
4	2	6.30 -4			B10 43	\		17	Co	133			
4	3	2.52 -3			B11 49	> 5%-B Poly	18	Pb	349				
4	-4	3.97 -2			C 55	/		19	N	61			
5	7	5.643 -2			Al 91 \			20	Mn	157			
5	20	4.1712-4			Mn 157 \			21	Cr	151			
5	16	2.622 -3			Mg 85 > Al 5083								
5	-21	8.930 -5			Cr 151 /								
6	9	1.67 -2			W182 301 \								
6	10	9.06 -3			W183 307 \								
6	11	1.94 -2			W184 313 > Tungsten								
6	-12	1.81e-2			W186 319 /								
7	1	7.94 -2			H 1 > Polyethylene								
7	-4	3.97 -2			C 55 /								
8	1	5.845 -2			H \								
8	13	5.588 -2			Li6 25 > LiH 95.6% enriched								
8	-14	2.572 -3			Li7 31 /								

Appendix E: Material Densities and Element Number Densities

Table 12: Material and Element Number Densities

Material	Material Density (g/cc)	Elements	Atom Density (atoms per barn-cm)
High Density Polyethylene	0.95 ^a	Carbon Hydrogen	3.96x10 ⁻² 7.94x10 ⁻²
5% Boron Polyethylene	0.98 ^b	Carbon Hydrogen Boron-10 Boron-11	3.97x10 ⁻² 7.94x10 ⁻² 6.30x10 ⁻⁴ 2.52x10 ⁻³
Lead Borated Polyethylene	4.2 ^c	Lead Carbon Oxygen Hydrogen Calcium Boron-10 Boron-11 Silicon Sodium Magnesium Aluminum	9.928x10 ⁻³ 2.165x10 ⁻² 5.693x10 ⁻³ 4.266x10 ⁻² 6.689x10 ⁻⁴ 4.679x10 ⁻⁴ 1.965x10 ⁻³ 3.692x10 ⁻⁴ 3.741x10 ⁻⁴ 1.977x10 ⁻⁴ 4.687x10 ⁻⁵
Kapton	1.42 ^d	Carbon Hydrogen Oxygen Nitrogen	4.8169x10 ⁻² 3.9427x10 ⁻² 1.0952x10 ⁻² 4.3808x10 ⁻³
Aluminum 5083	2.69 ^e	Aluminum Manganese Magnesium Chromium	5.643x10 ⁻² 4.171x10 ⁻⁴ 2.622x10 ⁻³ 8.930x10 ⁻⁵
Liquid Helium	0.125 ^f	Helium	1.869x10 ⁻²
Liquid Methane	0.424 ^g	Carbon Hydrogen	1.597x10 ⁻² 6.391x10 ⁻²
Liquid Hydrogen	0.071 ^h	Hydrogen	4.240x10 ⁻²
Tungsten	19.35 ⁱ	Tungsten 182 Tungsten 183 Tungsten 184 Tungsten 186	1.667x10 ⁻² 9.064x10 ⁻³ 1.944x10 ⁻² 1.813x10 ⁻²
Enriched Lithium Hydride	0.686	Hydrogen Lithium 6 Lithium 7	5.845x10 ⁻² 5.588x10 ⁻² 2.572x10 ⁻³

^a[Daniels, 1989:72], ^b[Shielding and Foils, 1982:12],
^c[Tobin, 1991], ^d[Shrinet, 1982:557], ^e[American Society for
Metals, 1978:113], ^f[Compressed Gas Association, 1990:388],
^g[Weast, 1988:B-330], ^h[Compressed Gas Association,
1990:395], ⁱ[GE Nuclear Energy, 1989:16]

Appendix F: Photon Detector Response Functions

Table 13: Photon Detector Response Functions (Silicon)

Upper Energy (eV)	Lower Energy (eV)	Ave Energy (eV)	Dose Response (Gy/photon/cm^2)	Energy Response (J/photon)
2.00E+07	1.40E+07	1.70E+07	8.5045E-10	2.7234E-12
1.40E+07	1.20E+07	1.30E+07	1.5823E-09	2.0826E-12
1.20E+07	1.00E+07	1.10E+07	2.4318E-09	1.7622E-12
1.00E+07	8.00E+06	9.00E+06	1.9441E-09	1.4418E-12
8.00E+06	7.00E+06	7.50E+06	2.485E-09	1.2015E-12
7.00E+06	6.00E+06	6.50E+06	2.175E-09	1.0413E-12
6.00E+06	5.00E+06	5.50E+06	1.862E-09	8.811E-13
5.00E+06	4.00E+06	4.50E+06	1.545E-09	7.209E-13
4.00E+06	3.00E+06	3.50E+06	1.222E-09	5.607E-13
3.00E+06	2.50E+06	2.75E+06	9.803E-10	4.4055E-13
2.50E+06	2.00E+06	2.25E+06	8.284E-10	3.6045E-13
2.00E+06	1.50E+06	1.75E+06	6.718E-10	2.8035E-13
1.50E+06	1.00E+06	1.25E+06	5.074E-10	2.0025E-13
1.00E+06	7.00E+05	8.50E+05	3.681E-10	1.3617E-13
7.00E+05	4.50E+05	5.75E+05	2.657E-10	9.2115E-14
4.50E+05	3.00E+05	3.75E+05	1.841E-10	6.0075E-14
3.00E+05	1.50E+05	2.25E+05	1.12E-10	3.6045E-14
1.50E+05	1.00E+05	1.25E+05	7.454E-11	2.0025E-14
1.00E+05	7.00E+04	8.50E+04	8.359E-11	1.3617E-14
7.00E+04	4.50E+04	5.75E+04	1.447E-10	9.2115E-15
4.50E+04	3.00E+04	3.75E+04	3.211E-10	6.0075E-15
3.00E+04	2.00E+04	2.50E+04	7.3881E-10	4.005E-15
2.00E+04	1.00E+04	1.50E+04	2.26E-09	2.403E-15

Appendix G: Neutron Detector Response Functions

Table 14: Neutron Detector Response Functions

Upper Energy (eV)	Lower Energy (eV)	Ave Energy (eV)	Dose Response (Gy/n/cm ²)	Energy Response (J/neutron)
1.96E+07	1.69E+07	1.83E+07	1.4136E-09	2.92365E-12
1.69E+07	1.49E+07	1.59E+07	1.1867E-09	2.54718E-12
1.49E+07	1.42E+07	1.46E+07	1.138E-09	2.33091E-12
1.42E+07	1.38E+07	1.40E+07	1.1213E-09	2.2428E-12
1.38E+07	1.28E+07	1.33E+07	1.1108E-09	2.13066E-12
1.28E+07	1.22E+07	1.25E+07	1.0931E-09	2.0025E-12
1.22E+07	1.11E+07	1.17E+07	1.056E-09	1.86633E-12
1.11E+07	1.00E+07	1.06E+07	9.6552E-10	1.69011E-12
1.00E+07	9.00E+06	9.50E+06	8.2573E-10	1.5219E-12
9.00E+06	8.20E+06	8.60E+06	7.1892E-10	1.37772E-12
8.20E+06	7.40E+06	7.80E+06	6.4233E-10	1.24956E-12
7.40E+06	6.40E+06	6.90E+06	3.9406E-10	1.10538E-12
6.40E+06	5.00E+06	5.70E+06	1.7265E-10	9.1314E-13
5.00E+06	4.70E+06	4.85E+06	1.3041E-10	7.7697E-13
4.70E+06	4.10E+06	4.40E+06	9.9411E-11	7.0488E-13
4.10E+06	3.00E+06	3.55E+06	6.4401E-11	5.6871E-13
3.00E+06	2.40E+06	2.70E+06	5.83434E-11	4.3254E-13
2.40E+06	2.30E+06	2.35E+06	4.9385E-11	3.7647E-13
2.30E+06	1.80E+06	2.05E+06	5.0306E-11	3.2841E-13
1.80E+06	1.42E+06	1.61E+06	4.0888E-11	2.58138E-13
1.42E+06	1.10E+06	1.26E+06	2.2068E-11	2.02068E-13
1.10E+06	9.62E+05	1.03E+06	2.2945E-11	1.65137E-13
9.62E+05	8.21E+05	8.91E+05	2.6028E-11	1.42777E-13
8.21E+05	7.43E+05	7.82E+05	2.5167E-11	1.25244E-13
7.43E+05	6.39E+05	6.91E+05	1.4525E-11	1.107E-13
6.39E+05	5.50E+05	5.95E+05	1.9371E-11	9.52613E-14
5.50E+05	3.69E+05	4.59E+05	1.2283E-11	7.35983E-14
3.69E+05	2.47E+05	3.08E+05	1.0185E-11	4.93472E-14
2.47E+05	1.60E+05	2.04E+05	1.1136E-11	3.26199E-14
1.60E+05	1.10E+05	1.35E+05	5.3753E-13	2.1627E-14
1.10E+05	5.20E+04	8.10E+04	7.6044E-13	1.29762E-14
5.20E+04	3.43E+04	4.32E+04	4.0843E-13	6.91319E-15
3.43E+04	2.50E+04	2.97E+04	2.5145E-13	4.75049E-15
2.50E+04	2.19E+04	2.34E+04	1.9299E-13	3.75469E-15
2.19E+04	1.00E+04	1.59E+04	1.3058E-13	2.55319E-15
1.00E+04	3.40E+03	6.70E+03	5.7105E-14	1.07334E-15
3.40E+03	1.20E+03	2.30E+03	1.7532E-14	3.6846E-16
1.20E+03	5.80E+02	8.90E+02	6.5553E-15	1.42578E-16
5.80E+02	2.75E+02	4.28E+02	2.7522E-15	6.85143E-17
2.75E+02	1.00E+02	1.88E+02	3.1906E-15	3.00663E-17
1.00E+02	2.90E+01	6.45E+01	1.5852E-15	1.03329E-17
2.90E+01	1.10E+01	2.00E+01	5.8717E-16	3.204E-18
1.10E+01	3.10E+00	7.05E+00	2.5149E-16	1.12941E-18
3.10E+00	1.10E+00	2.10E+00	2.7854E-16	3.3642E-19
1.10E+00	4.14E-01	7.57E-01	7.557E-16	1.21271E-19
4.14E-01	1.00E-05	2.07E-01	8.8589E-16	3.31622E-20

Vita

Captain Jeffrey E. Malapit was born on 25 December 1960 in Bethesda, Maryland. He attended the United States Military Academy at West Point, New York, graduating with a Bachelor of Science in May 1983 and a regular commission in the U.S. Army. Following graduation, he attended the U.S. Army Engineer Officer Basic Course and Atomic Demolition and Munitions Course at Fort Belvoir, Virginia. He served his first tour of duty as a combat engineer platoon leader of 35 soldiers, then company executive officer of 89 soldiers with the 13th Engineer Battalion, 7th Infantry Division (Light), the first light combat engineer battalion in the Army force structure. In 1987, Captain Malapit attended the U.S. Army Engineer Officer Advanced Course, graduated as a distinguished graduate, then was selected to serve as a platoon trainer for 52 newly commissioned engineer lieutenants. He served with the 23rd Engineer Battalion, 3rd Armored Division in Hanau, Germany as the Battalion Intelligence Officer in November 1987, then as the commander of a 165 man combat engineer company in February 1989. Following his command, he entered the School of Engineering, Air Force Institute of Technology, in August 1990. Captain Malapit is a registered professional engineer licensed in the Commonwealth of Virginia since 1987.